TRIBHUVAN UNIVERSITY
INSTITUTE OF ENGINEERING
PULCHOWK CAMPUS

B-10-BME-2019-2024

Experimental Analysis on Vapour Compression Refrigeration System

by

Jeena Shrestha (076BME015)
Niraj Thapa (076BME024)
Rejisha Pradhan (076BME032)
Sujit Sah Baniya (076BME046)

A FINAL DEFENSE REPORT

SUBMITTED TO THE DEPARTMENT OF MECHANICAL AND AEROSPACE ENGINEERING IN PARTIAL FULFILLMENT OF THE REQUIREMENTS FOR THE DEGREE OF BACHELOR IN MECHANICAL ENGINEERING

DEPARTMENT OF MECHANICAL AND AEROSPACE ENGINEERING
LALITPUR, NEPAL

APRIL 2024

COPYRIGHT

Head of Department
Department of Mechanical and Aerospace Engineering
Central Campus Pulchowk, Institute of Engineering
Lalitpur, Kathmandu
Nepal

LETTER OF APPROVAL

The undersigned certify that they have read, and recommended to the Institute of Engineering for acceptance, a project report entitled "**Experimental Analysis on Vapour Compression Refrigeration System**" submitted by **Jeena Shrestha, Niraj Thapa, Rejisha Pradhan, Sujit Sah Baniya** in partial fulfilment of the requirements for the Bachelor's Degree in Mechanical Engineering.

Supervisor: **Vishwa Prasanna Amatya**
Associate Professor
Department of Mechanical and Aerospace Engineering
Institute of Engineering, Pulchowk Campus

External Examiner: **Er. Rudra Mani Ghimire**
Deputy Manager
Civil Aviation Authority of Nepal

Tribhuvan University
Institute of Engineering
Department of Mechanical and Aerospace Engineering
Pulchowk Campus

Head of Department: **Sudip Bhattarai (PhD)**
Assistant Professor
Department of Mechanical and Aerospace Engineering
Institute of Engineering, Pulchowk Campus

2024-04-09

Date of Approval:

ABSTRACT

Vapour Compression Refrigeration system (VCRs) has been extensively used in Refrigeration and HVAC sectors due to its beneficial characteristics like higher COP and Refrigerating Effect. However, these sectors and consequently VCRs contribute to a substantial and rapidly increasing global energy consumption which has raised huge concerns. This project aimed to experimentally analyse the vapour compression refrigeration system and compare performance of the system with and without heat addition. It was conducted by fabricating a VCR unit and adding extra heat to the unit before and after the compression process. The COP of the system increased by 46.07% when heat was added before compressor while the current consumption of the compressor decreased by 12.07%. However, COP of the system decreased by 22.7% when heat was added to the system after compressor with 32.6% increase in current consumption.

ACKNOWLEDGEMENTS

We are grateful to the Department of Mechanical and Aerospace Engineering for giving us the opportunity and platform to conduct this project. We extend our sincere appreciation to our Head of Department, Asst. Professor Dr. Sudip Bhattarai for providing invaluable support and resources, which were essential for the successful completion of our project. We are deeply indebted to our supervisor, Associate Professor Vishwa Prasanna Amatya for his invaluable guidance and unwavering support for this project. His expertise and constructive feedback have been instrumental for our project. We are also thankful to Asst. Professor Navin Kumar Jha for his prompt and insightful responses to our inquiries. We would like to express our sincere gratitude to the Campus Carpentry team and Mechanical Workshop for allowing us to use their tools.

We extend our sincere appreciation to Bal Purshottam Shakya for providing us the resources necessary for the fabrication process of our project. Additionally, our heartfelt thanks go to our classmate Bibek Shrestha for lending us the necessary mechanical tools, contributing to the successful execution of our project.

TABLE OF CONTENTS

LIST OF FIGURES

LIST OF TABLES

LIST OF ACRONYMS AND ABBREVIATIONS

AC	Air Conditioning
BC	Before Christ
COP	Coefficient of Performance
EES	Engineering Equation Solver
HP	Horsepower
HVAC	Heating Ventilation and Air-Conditioning
IEA	International Energy Agency
LBP	Low Back Pressure
LLSL-HX	Liquid Line Suction Line Heat Exchanger
LP	Low Pressure
PVT. Ltd	Private Limited
SL-HX	Suction Line Heat Exchanger
VCRs	Vapour Compression Refrigeration System

LIST OF SYMBOLS

η_e	Electrical Efficiency
γ	Heat Capacity Ratio
$\dot{m}$	Mass flow rate
η_m	Mechanical Efficiency
C_p	Specific Heat Capacity at constant pressure
C_v	Specific Heat Capacity at constant volume
η_v	Volumetric Efficiency

CHAPTER ONE: INTRODUCTION

1.1 Background

Understanding the historical context of refrigeration sets the stage for a closer examination of the vapour compression refrigeration system. This system's significance lies in its widespread utilization, playing important role in both comfort and process air conditioning.

1.1.1 History and development of Refrigeration

Refrigeration, broadly defined as any method that maintains a temperature lower than the ambient surroundings, has a history dating back to ancient times, including ice houses in Mesopotamia (1780 BC) and Persian Yakhchals (400 BC). In the 1800s, natural ice harvesting was a thriving part of the economy, with large quantities stored in insulated ice houses. Mechanical refrigeration systems, using various refrigerants like sulphur dioxide, methyl chloride, ether, and carbon dioxide, were invented during this time. Some systems in the early 1900s utilized carbon dioxide as a refrigerant, requiring cold condenser water. In the 1930s, CO2 was used in cascade systems with ammonia for freezing food. Ammonia absorption systems were viable until the 1950s and 1960s, utilizing waste heat. Reciprocating compressors, refined in the early 1900s, saw improvements in the late 1930s with the development of v/w-type compressors. The 1950s and 1960s witnessed a significant expansion in the frozen food industry, leading to increased demand for rotary and v/w compressors. In the late 1960s, the helical screw compressor, invented in Sweden in 1935, became widely used for high-pressure refrigerants [1].

1.1.2 Vapour Compression Refrigeration System

In vapour compression refrigeration systems, compressors increase the refrigerant's pressure and temperature levels after the refrigerating effect is produced. The compressed refrigerant releases heat to the sink and undergoes condensation, transforming into a liquid state. This liquid refrigerant is subsequently expanded to a low-pressure, low-temperature vapour, generating a refrigerating effect during evaporation. Vapour compression systems are extensively utilised in both comfort and process air conditioning, representing the employed refrigeration systems [2].

1.1.3 Components of vapour compression refrigeration system

Compressor, condenser, throttling device, evaporator, drier are the main components of vapour compression refrigeration systems.

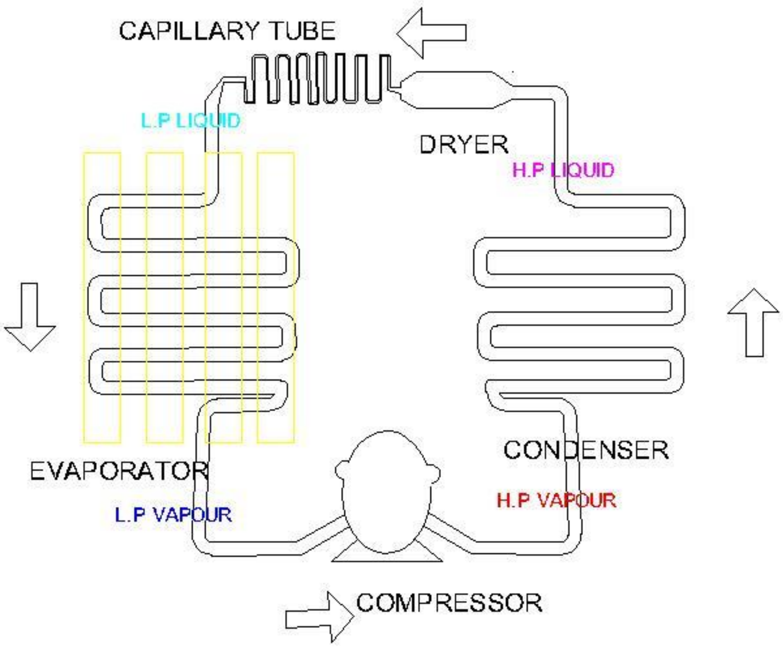

Fig 1.1: vapour compression refrigeration cycle

1.1.3.1 Compressor

Compressor is a device that is used to compress the refrigerant to increase its pressure and temperature. Low pressure and temperature gas gets compressed into high pressure and temperature gas in the compressor. Different types of compressors can be used in VCRs depending on the size of refrigeration system and volume of refrigerant. Centrifugal, reciprocating, screw, scroll etc. are types of compressors that can be used in VCRs [3].

1.1.3.2 Condenser

Condenser is placed at the discharge side of the compressor. It cools down the high temperature vapour refrigerant coming from the compressor by allowing the hot refrigerant to release its latent heat to the surrounding. When high pressure gas enters into the condenser it gets condensed and changes its phase to high pressure liquid [3].

1.1.3.3 Filter Dryer

It is used to remove moisture and particles from refrigerants before it enters into an expansion device.

1.1.3.4 Capillary Tube

The capillary tube serves as a widely used expansion device in household refrigeration systems. Typically, these tubes have diameters ranging from 0.5 mm to 2.0 mm and lengths spanning 2 m to 6 m. Capillary tubes have several advantages over expansion devices like thermostatic expansion valves. They are simple, cost-effective, and have ability to equalise pressure during off-cycle enabling the compressor to start with low torque [4].

1.1.3.5 Evaporator

Evaporator is a heat exchanger that enables the refrigerant to remove heat from the desired space. Evaporator is placed after the capillary tube and before the compressor in the refrigeration system. It usually has a series of coils that increases its surface area and aids in the heat transfer process. The low-pressure liquid refrigerant in the evaporator absorbs heat from the refrigerated space and consequently evaporates into a low-pressure vapour. It utilises the latent heat for the refrigeration process [3].

1.1.4 Thermodynamics Cycles of VCRs

In a vapour compression refrigeration system, refrigerant is circulated in a closed loop and heat transfer takes place by changing the phase of refrigerant. The ideal thermodynamic cycle of VCRs is shown in Fig:1.2 and Fig:1.3. The four-process involved in an ideal VCR cycle are:

Process 1-2: Isentropic Compression

Process 2-3: Isobaric Heat Rejection in Condenser

Process 3-4: Throttling in Expansion valve (Capillary Tube)

Process 4-1: Isobaric Heat Addition in Evaporator

However, in the actual process compression will not be isentropic due to the presence of irreversibilities like friction loss, pressure drop, heat transfer to the surroundings, etc. The actual thermodynamic process of VCRs is shown in Fig: 1.4 and Fig: 1.5.

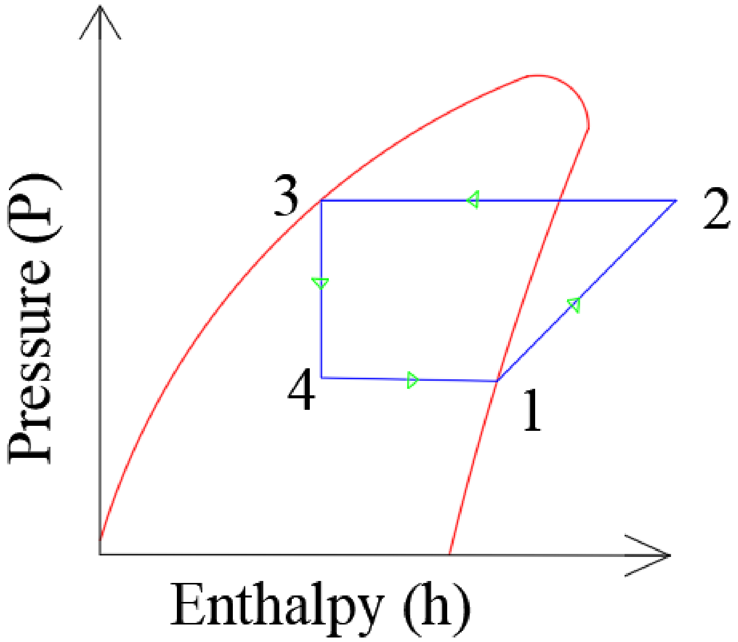

Fig 1.2: Ideal Refrigeration Cycle on P-h diagram

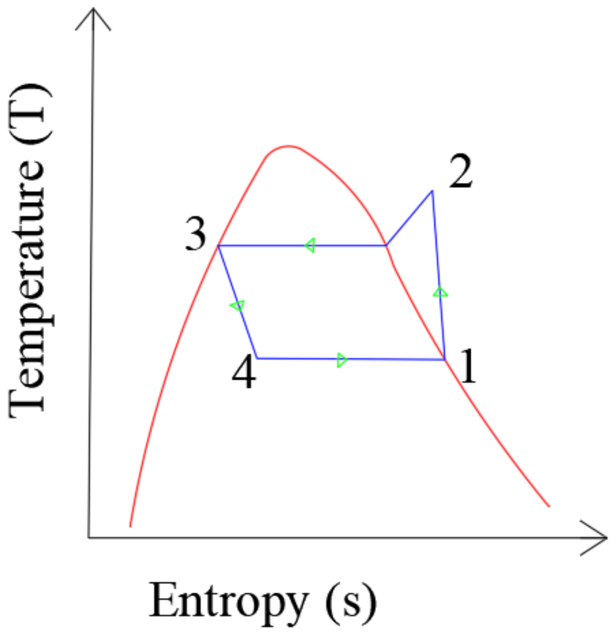

Fig 1.3: Ideal Refrigeration Cycle on T-s diagram

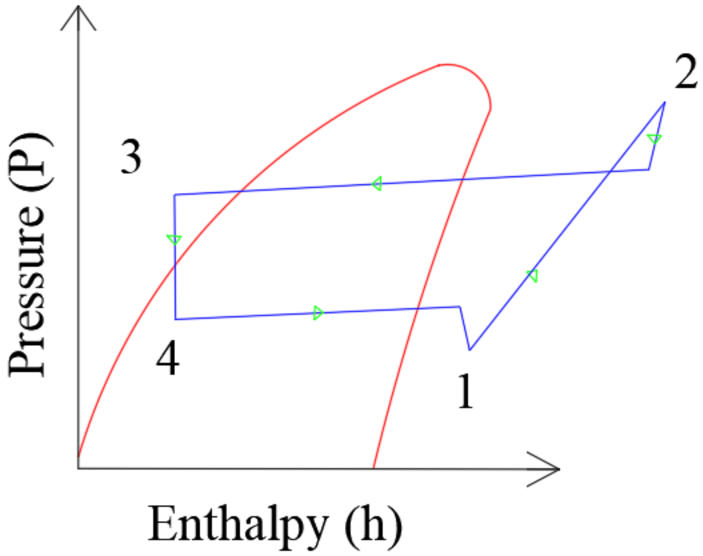

Fig 1.4: Actual Refrigeration Cycle on P-h diagram

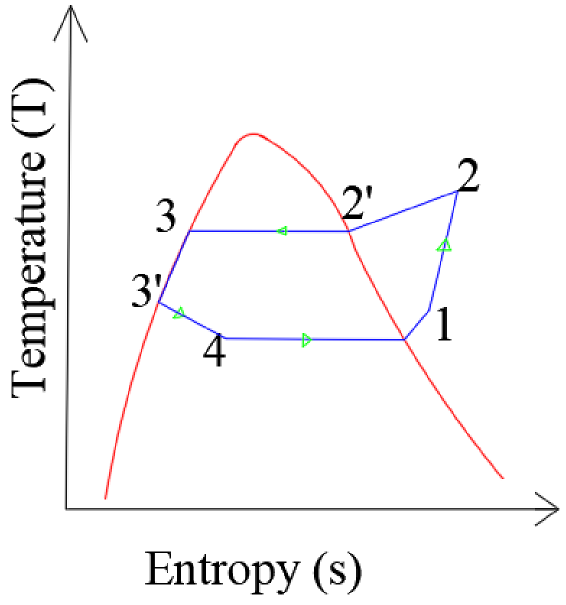

Fig 1.5: Actual Refrigeration Cycle on T-s diagram

1.2 Problem Statement

Vapour Compression system is extensively used for Refrigeration and HVAC sector for space cooling, space heating, cold storage etc. The HVAC system accounts for 40% of the total building energy consumption and about 16% of the global energy consumption [5]. With the world experiencing extreme temperatures in recent years the energy demand for the HVAC system can only increase tremendously. As per, latest IEA data, sales of HVAC equipment were increased by 11 % as of 2022 and further increments have been predicted [6]. Similarly, the IEA also warns that the electricity demand for space cooling can reach as much as 40% globally by 2030 without the move towards better products [7]. This rapidly growing energy need raises concerns over supply difficulties and exhaustion of energy resources and demands for improvement in the efficiency of the vapour compression refrigeration system.

This project aims to experimentally analyse the vapour compression refrigeration system and compare performance of the system with and without heat addition. This has the potential to increase efficiency of VCRs and reduce the impact HVAC and refrigeration systems have on global energy use.

1.3 Objectives

1.3.1 Main Objective

The main objective of this project is to fabricate the vapour compression refrigeration system and experimentally study it by conducting performance analysis of system with and without heat addition before and after the compression process.

1.3.2 Specific Objectives

i. To select components of appropriate size for VCRs

ii. To fabricate Vapour Compression Refrigeration System

iii. To select components of appropriate size for the heat addition process

iv. To analyse and compare the performance of VCRs with and without heat addition before and after the compressor.

CHAPTER TWO: LITERATURE REVIEW

2.1 COP of Refrigeration cycle

The coefficient of performance (COP) of a VCRs gives us the measures of the efficiency of the system. It is the ratio of the cooling produced by the evaporator to the amount of work or energy input utilised by the system. Greater Coefficient of Performance (COP) values correspond to increased efficiency, reduced energy (power) consumption, and consequently, decreased operating expenses [3].

Usually, the work input to the VCRs is electrical energy. So, it can also be measured by

$$COP = \frac{Refrigerating\ Effect}{Work\ done}$$

The coefficient of performance (COP) of VCRs is calculated practically by measuring the cooling or heating effect produced by the system and the electrical energy consumed by the compressor. The general steps taken to calculate the COP of VCRs used for cooling are:

i. We can measure the cooling effect produced by the system by measuring the amount of heat removed from the maintained refrigerated space per unit time. This can be done using a heat flow metre or by measuring the change in temperature of a known mass of water or another suitable medium and with their specific heat capacity known to us.

ii. Then we can measure the electricity consumption of the VCRs over a specific amount of time [8].

2.2 Factor affecting COP of refrigeration cycle

COP of refrigeration cycle varies due to various factors such as inlet and outlet pressure of compressor, temperature difference between indoor and outdoor, superheat and subcooled process etc. [3,9,10].

2.2.1 Effect of Suction Pressure

When there is decrease in suction pressure due to losses during flow of refrigerant, refrigerating effect decreases, compressor work input increases. Thus, the COP of the system decreases [3].

2.2.2 Effect of Discharge Pressure

When there is increase in discharge pressure due to losses during flow of refrigerant, refrigerating effect decreases, compressor work input increases. Thus, the COP of the system decreases [3].

2.2.3 Effect of Evaporator Temperature

When there is increase in evaporator temperature, there is reduction in compressor work due to decrease in pressure ratio of compressor. However, refrigerating capacity is increased due to increased heat transfer between refrigerant and medium being cooled. The combined effect of these two factors results in overall increment of COP of the system [9, 10].

2.2.4 Effect of Condenser Temperature

With increase in condenser temperature, the effect is just opposite to that of evaporator temperature rise. As condenser temperature increases, the COP of the system decreases [9,10].

2.2.5 Effect of Superheating

Superheating refrigerant before suction increases the refrigerating effect of the system, hence increasing COP [11].

2.2.6 Effect of Subcooling

Subcooling refrigerant increases refrigerating effect, thus increasing COP of the system [11].

2.3 Method of Increasing COP of VCR Cycle by Regenerative method

During the 69th conference of the Italian Thermal Engineering (ATI 2014), a paper was presented by Ascani Maurizio, Cerri Giovanni, and De Francesco Eduardo, the focus of which was the optimization of power consumption in a cooling plant layout. The proposed approach involved a compressor expander group to increase pressure at the main compressor's inlet. The feasibility test using R-404a demonstrated positive results, indicating an expected increase in the coefficient of performance (COP) by approximately 22-23% [12].

Additionally, Sobhit Mishra and Nomendra Tomar presented a theoretical analysis during the same conference. Their research centred on a new regenerative compression system incorporating an ejector as the second stage of compression. The theoretical analysis showcased promising outcomes, revealing a performance increase of 22% for R-134a and 11.7% for R-1234yf in the regenerative cycle. These findings contribute valuable insights to the advancement of energy-efficient and optimised cooling systems [13].

2.4 Method of Increasing COP of AC by Heat Addition

In VCRs, most power is consumed by the compressor while circulating refrigerant. Compression process can be enhanced by adding extra heat to the refrigerant before the compressor inlet [14]. LLSL-HX is used to transfer heat from the condenser section of VCRs to heat refrigerant in the suction line of the compressor. In an experiment conducted by Prasanna & Kishore in 2014 it was found that using the LLSL-HX refrigeration effect of the VCR cycle was increased by 16% and the workload of the compressor was reduced by 14% [15]. Alli et al, increased the COP of vehicle air conditioning systems by 10% using SL-HX in their experiment [16].

2.5 Effect of Ambient Temperature on COP

Ambient Temperature and relative humidity have significant impact on COP and power consumption of Vapour compression refrigeration system. With constant relative humidity, change in power consumption is proportional to change in ambient temperature and with increase in ambient temperature, COP of refrigeration system decreases [17].

As per experiment conducted in [18], for every one-degree Celsius rise in temperature compressor work input is increased by 0.017 kW linearly and cooling capacity is decreased by 0.022 kW.

2.6 P-h chart

The p-h chart is the most convenient diagram for examining the characteristics of a refrigerant. In this chart, vertical axes depict pressure, while horizontal axes represent enthalpy (total heat). At the critical point, the saturated liquid line and saturated vapour line converge. A saturated liquid refers to one with a temperature matching its pressure's saturation temperature. Consequently, the area to the left of the saturated liquid line is the sub-cooled liquid region. The space between the liquid and vapour lines is termed the wet vapour region, and to the right of the saturated vapour line lies the superheated vapour region [3].

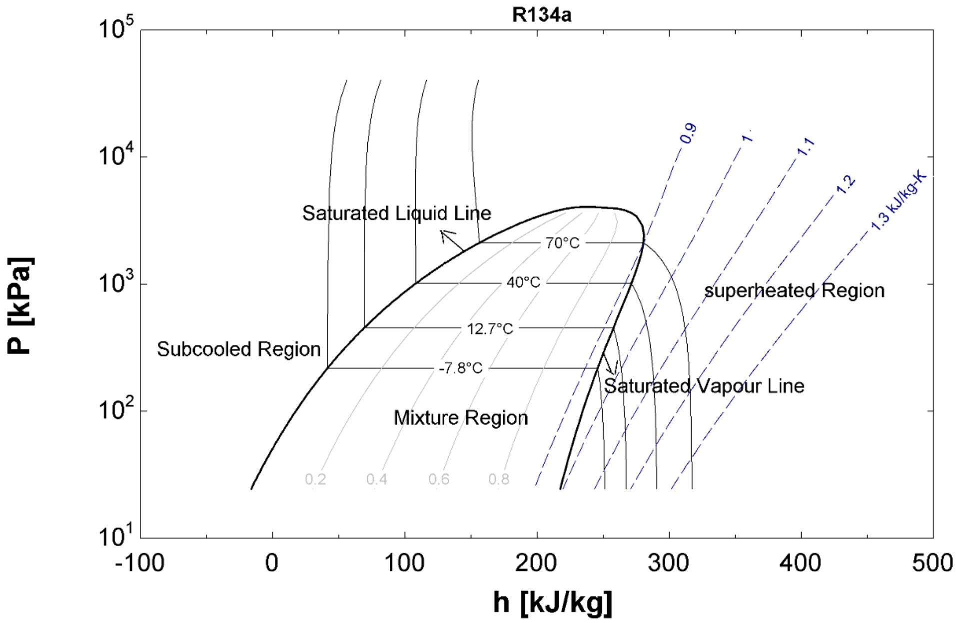

Fig 2.1: Pressure-Enthalpy Chart

2.7 Refrigerant R- 134a

A refrigerant is the fluid in a refrigeration system, responsible for absorbing and conveying heat. It absorbs heat at low temperature and pressure, releasing it at higher temperature and pressure. Refrigerants typically undergo phase changes during heat absorption (evaporation) and heat release (condensation). R134a (1,1,1,2-Tetrafluoroethane) is a hydrofluorocarbon refrigerant. R134a is widely employed in refrigeration applications as azeotropic blend, owing to its essential attributes like nonflammability, chemical stability, and favourable thermodynamic properties, all of which have no detrimental impact on the ozone layer. [19]

2.8 Fabrication process

The fabrication processes used in the fabrication of our setup are explained below.

2.8.1 Cutting

Tube cutter is used to make straight cuts in copper pipes. The copper pipe is inserted securely into the cutting tool. Proper handling of the pipe is ensured to achieve satisfactory results. The lever is set to establish contact between the blade and the pipe. The tube cutter is rotated counter clockwise, completing one full turn until it is sensed that the blade is initiating the cutting process. Subsequently, the rotation is reversed in a clockwise direction. While turning clockwise, the lever is periodically adjusted until the pipe is fully cut [20].

2.8.2 Swaging

Swaging is a technique used to join two copper tube pieces of identical diameter by enlarging or elongating the end of one piece to accommodate the other, facilitating subsequent soldering or brazing of the joint. The swaged ends are usually cylindrical in shape. Typically, the length of the joint that encompasses the other corresponds approximately to the outer diameter of the tubing.

Swaging tools primarily utilise pressure to expand or widen the end of copper tubing. Various types of swaging tools are available for copper pipes, including spike-shaped punch tools, manual tube expanders, and feed screw tools akin to flaring bars. Notably, flaring tool kits often come equipped with swaging bits or die blocks that can transform the flaring bar into a swaging bar.

The swaging process is first started by preparing essential tools, such as a tube cutter, reamer, sand cloth, brush, flaring block, swaging tool, and hammer. The tube is then cut to the specified or desired length. Burrs are removed, and residues are cleaned from the tube using the reamer. The tube is placed in a flare block or anvil block with a hole matching the outer diameter of the tube, with the tube extending slightly above the block. The appropriate swaging punch is placed in the tube, and it is either struck with a hammer or forced slowly into the pipes through the means of screw to achieve the desired shape and length of the joint. The joint is assembled, ensuring smooth fitting of the tubes. Post-swaging, the tubing is inspected for cracks or defects, and if any are detected, the swage is cut off, and the process is restarted [20].

2.8.3 Flaring

Flaring refers to the process of creating a wider, funnel-shaped lip at the end of a soft metal tube, typically copper or aluminium. This flared end then fits securely onto a fitting, such as a male flare nut, to create a leak-proof connection. Flaring tools primarily utilise pressure to create the flared ends. The bar-type tool is the most widely used flaring tool for copper tubing, equipped with various holes to accommodate different pipe and tube sizes effectively.

The initial step involves precisely cutting the copper pipe to the desired length, a tube-cutting tool ensures smooth and even cuts. Measurements are marked on the pipe, and the cutting tool is securely attached, rotating around the pipe to create a circular groove for a precise cut. The loose ends are trimmed using a deburring blade on most pipe cutters. Then the pipe is placed in a flare form to ensure a secure hold and proper cutting without altering the diameter of the pipe. The nut that is nearest is tightened first before tightening the other nut and the yoke is adjusted. Then the reamer is placed on the flare form while making sure that the conical point is placed at the centre of the pipe. The reamer is then slowly tightened to the copper pipe through a screw. The flared end is then attached to a fitting such as a flared nut, creating a leak-proof seal. Successful flaring results in a 45-degree angle covering the fitting. The process should be repeated if there are any defects on the flared surface [20].

2.8.4 Brazing

Brazing is a metal joining process that entails applying heat and introducing a filler metal to join two metal pieces. The filler metal, with a lower melting point than the metals being joined, is introduced either beforehand or during the heating of the parts. The copper pipes in the HVAC and Refrigeration systems are usually joined by the brazing method. It is because brazing creates a strong and durable joint that can withstand the high pressure and temperature experienced in refrigeration systems. The capillary action of the molten brazing filler metal fills any minute gaps between the joining parts, ensuring a tight and lasting seal and preventing the leakage of the refrigerant.

The brazing process begins with the thorough preparation of metal parts, ensuring the removal of contaminants like dirt or rust. Subsequently, the parts are meticulously fit together, leaving a small gap to facilitate the flow of the filler metal. A flux is then applied to the joint area, protecting the metal surfaces from oxidation and aiding in impurity removal. The assembled parts undergo heating to a temperature above the filler metal's melting point but below that of the base metals, allowing the filler metal capillaries to flow into the joint and create a robust bond. The filler metal used has a melting point higher than solder but lower than the base metals being joined. The joined components are then allowed to cool gradually, solidifying the filler metal and ensuring the durability of the connection [20].

2.9 Testing

Various tests should be conducted to ensure that the designed and fabricated system are free of leakages to get good results. Important testing method are described below.

2.9.1 Nitrogen Flushing

Nitrogen Flushing is done after the complete fabrication of the system. It is the process of cleaning pipelines using nitrogen gas. Dry Nitrogen is used to purge certain contaminants from the system by connecting the nitrogen regulator to a line and allowing it to expel the contaminants through the other line, while isolating the compressor. While supplying the nitrogen, precaution should be given so as not to exceed the system's working pressure [21].

2.9.2 Bubble Test

Bubble Test is one of the most widely used leak detection tests used in HVAC systems. It is typically suitable to find large leakages in the system. The part to be tested is filled with soap water and whether there is formation of bubbles or not is noted. Formation of bubbles indicates the presence of leakage, so appropriate measures must be taken to remove the leakage [21].

2.9.3 Pressure Testing

Pressure testing involves applying a defined pressure to the piping system to identify potential leaks. The objective of pressure testing is to confirm the absence of leaks in the system before it becomes operational. Pressurised Nitrogen is passed through the refrigerant circuit and left there for 24 hours by sealing the openings of pipes. If there is no fluctuation or very little fluctuation in the pressure reading of the pressure gauge, then it indicates the absence of minor leakages [21].

2.9.4 Vacuuming

Vacuuming is done to remove nitrogen gas and moisture from the system before refrigerant is charged in the system [21].

2.10 Choking of a Capillary Tube

The refrigerant flow in the capillary tube undergoes a flash process, transitioning from liquid to vapor-liquid mixture due to the reduction in the pressure of the refrigerant. Beyond the flashing point, pressure drops rapidly due to two-phase friction and vapor acceleration, leading to a saturated liquid-vapor mixture. As pressure continues to drop, saturation temperature decreases and refrigerant quality increases until the refrigerant reaches the capillary tube exit. This results in the increase in velocity of the fluid due to the larger specific volume until it gains sonic velocity, where the Mach number becomes unity, and choked flow occurs. After the Mach number becomes unity, the refrigerant entropy achieves a peak value and further decrease in backpressure does not change the mass flow rate through the capillary [22].

Capillary tube blockage may also occur due to presence of moisture, which freeze up in tube when the temperature of capillary tube falls below 0℃, and due to presence of dust particles.

2.11 Safety Consideration for Heat addition

High pressure cut-out and low-pressure cutout can be used as safety device in refrigeration system. LP cutout, connected in compressor suction side, cut off the compressor when suction pressure falls below certain set value. HP cut out, connected in compressor discharge side, cut off the compressor when discharge pressure exceeds above pre-set value [23].

CHAPTER THREE: METHODOLOGY

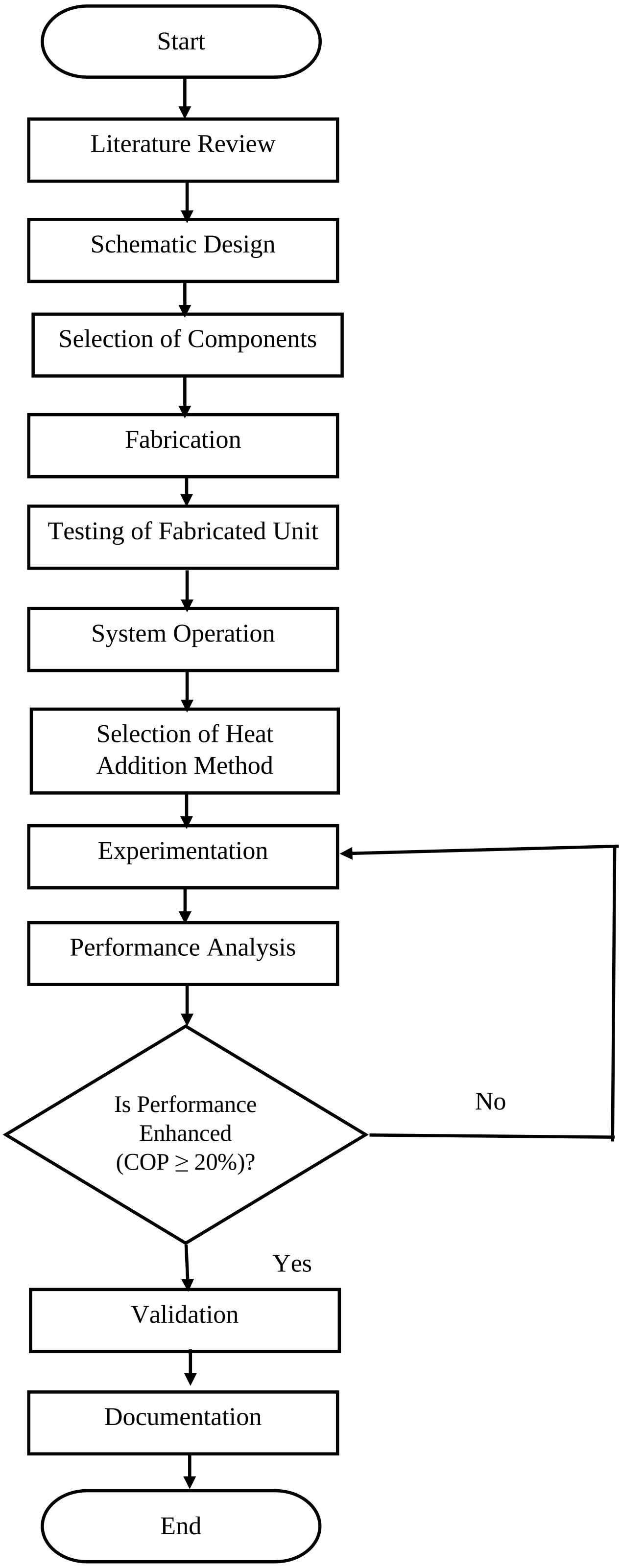

Fig 3.1: Methodology Flow Chart

3.1 Literature Review

By reviewing articles, books, journals and other sources, valuable knowledge and insights to conduct our project was gained. After a comprehensive review of the related literature the specifics of the experiment were decided. The performance of the Vapour Compression Refrigeration System by adding heat before and after the compressor was to be analysed against the normal system.

3.2 Materials

Different materials, tools, software that are necessary for our project are listed below

3.2.1 Equipment

i. Compressor
ii. Heat Exchangers
iii. Thermometers
iv. Pressure Gauges
v. Copper pipes
vi. Pipe fittings (elbow, tee, flare-nut)

3.2.2 Tools

i. Pipe cutter
ii. Flaring tools
iii. Brazing tools
iv. Wrenches
v. Drill machine
vi. Clamp Metre
vii. Wattmeter

3.2.3 Software Requirements

i. AutoCAD
ii. SolidWorks
iii. Microsoft 365
iv. Engineering Equation Solver (EES)

3.3 Schematic Design

As per the objective of our project, modifications were made on existing VCRs systems by adding heat exchangers before and after the compressor for the heat addition process. Then the simple schematic design of the experimental setup was prepared.

3.3.1 Normal Operation

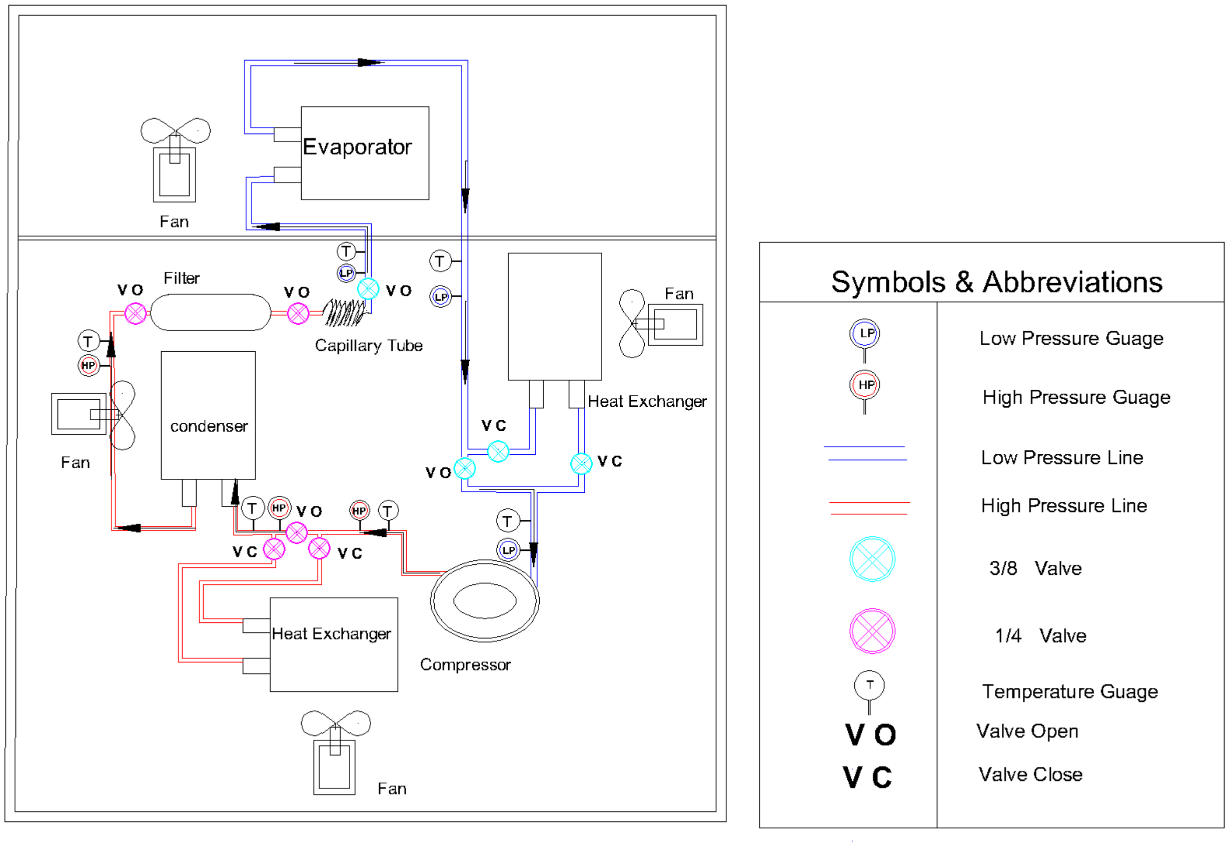

Fig 3.2: Schematic diagram of system for normal operation

3.3.2 Heat addition before compressor

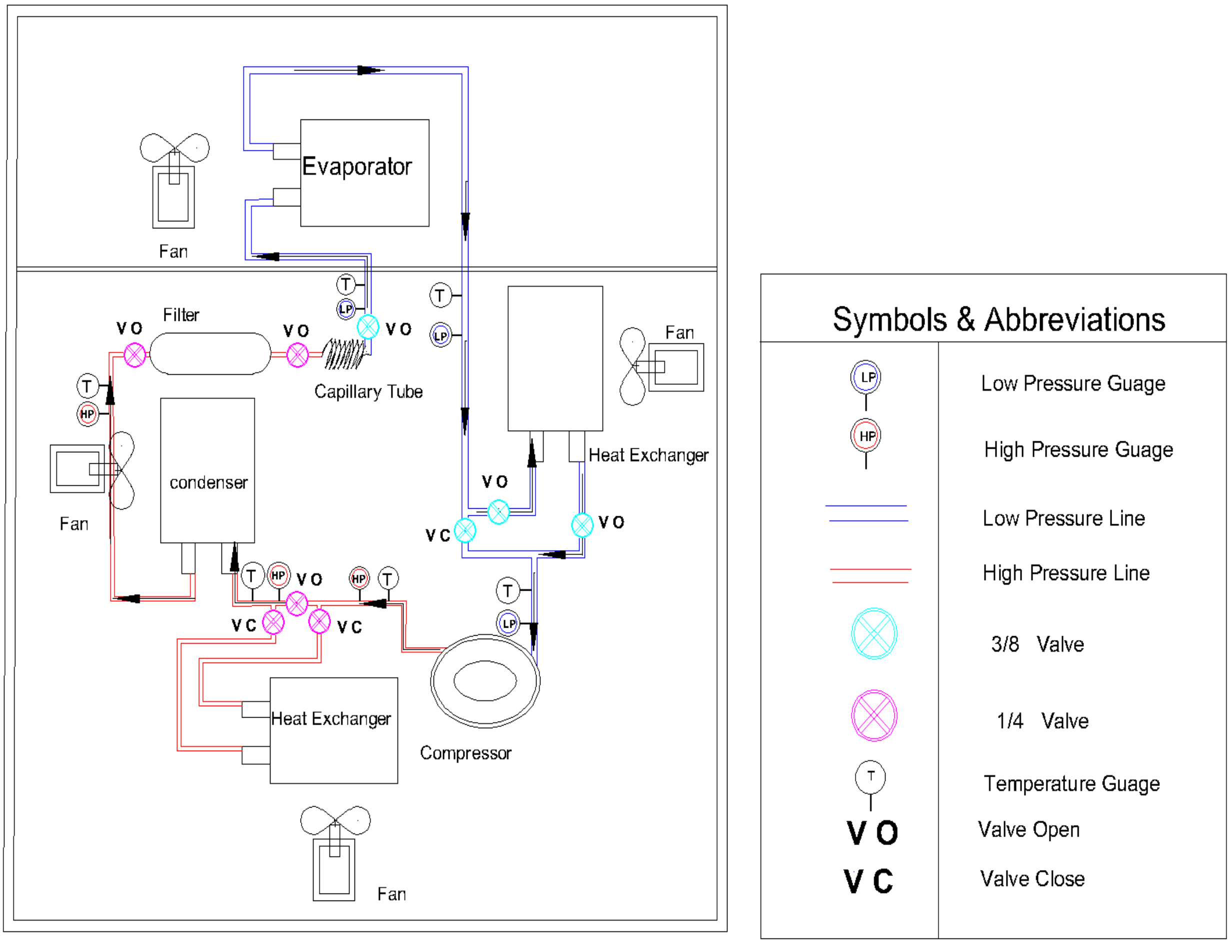

Fig 3.3: Schematic diagram of system for heat addition before compressor

3.3.3 Heat addition after compressor

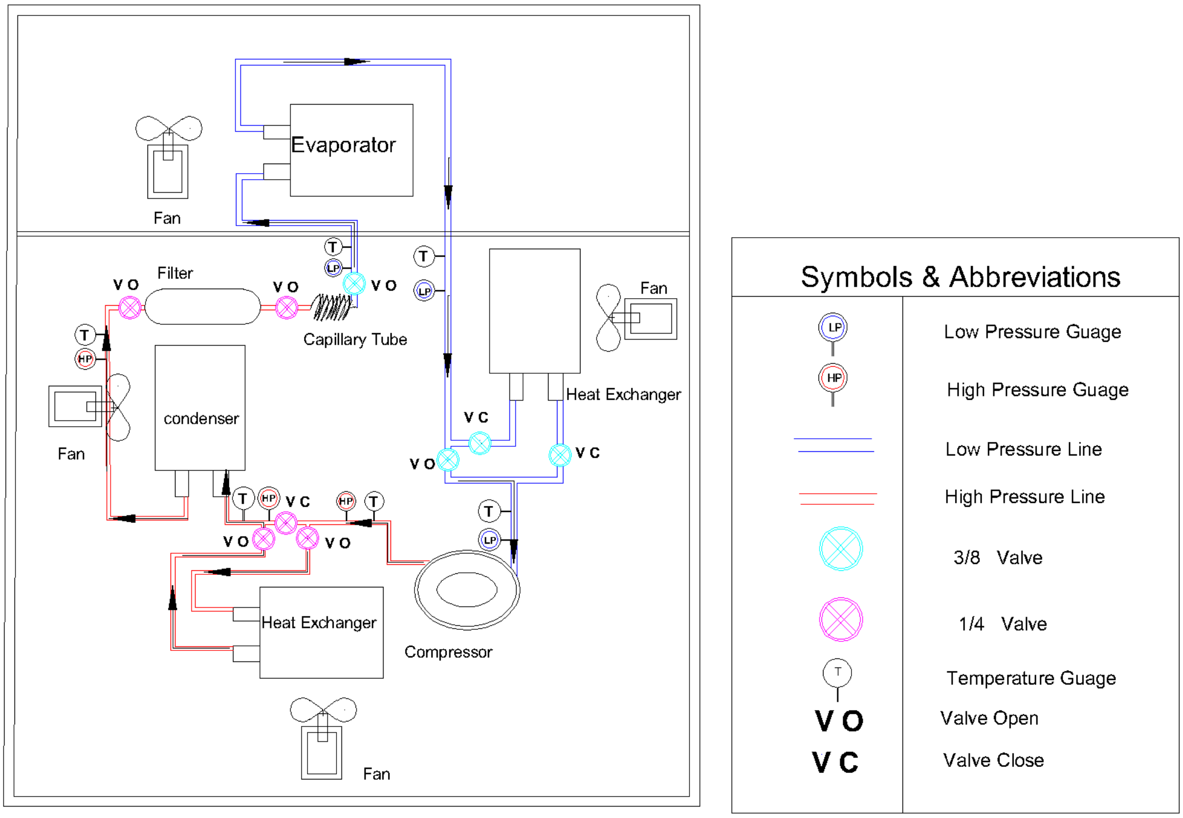

Fig 3.4: Schematic diagram of system for heat addition after compressor

3.4 Selection of components

Procedures followed for the selection of components are listed and described below

3.4.1 Selection of Compressor

Compressor was the component that was selected first for the fabrication of our VCR system. All the other components were then selected based on the compressor specifications and design requirements. The compressor that best suited the criteria of size, market availability and our budget was selected.

3.4.2 Selection of Condenser and Evaporator

For the selection of condenser, following procedures were consecutively followed.

3.4.2.1 Design Temperature

Initial design temperatures were taken under the guidelines of Compressor's data sheet.

Table 3.1: Design Temperatures

Suction Temperature (T_1)	-10℃
Discharge Temperature (T_2)	55℃
Condensing Temperature (T_3)	46℃
Evaporating Temperature (T_4)	-10℃

3.4.2.2 Plotting on P-h chart

After the design temperatures were obtained, respective temperatures were plotted in the P-h chart of R-134a, assuming ideal VCR cycle, to obtain necessary data for further calculations.

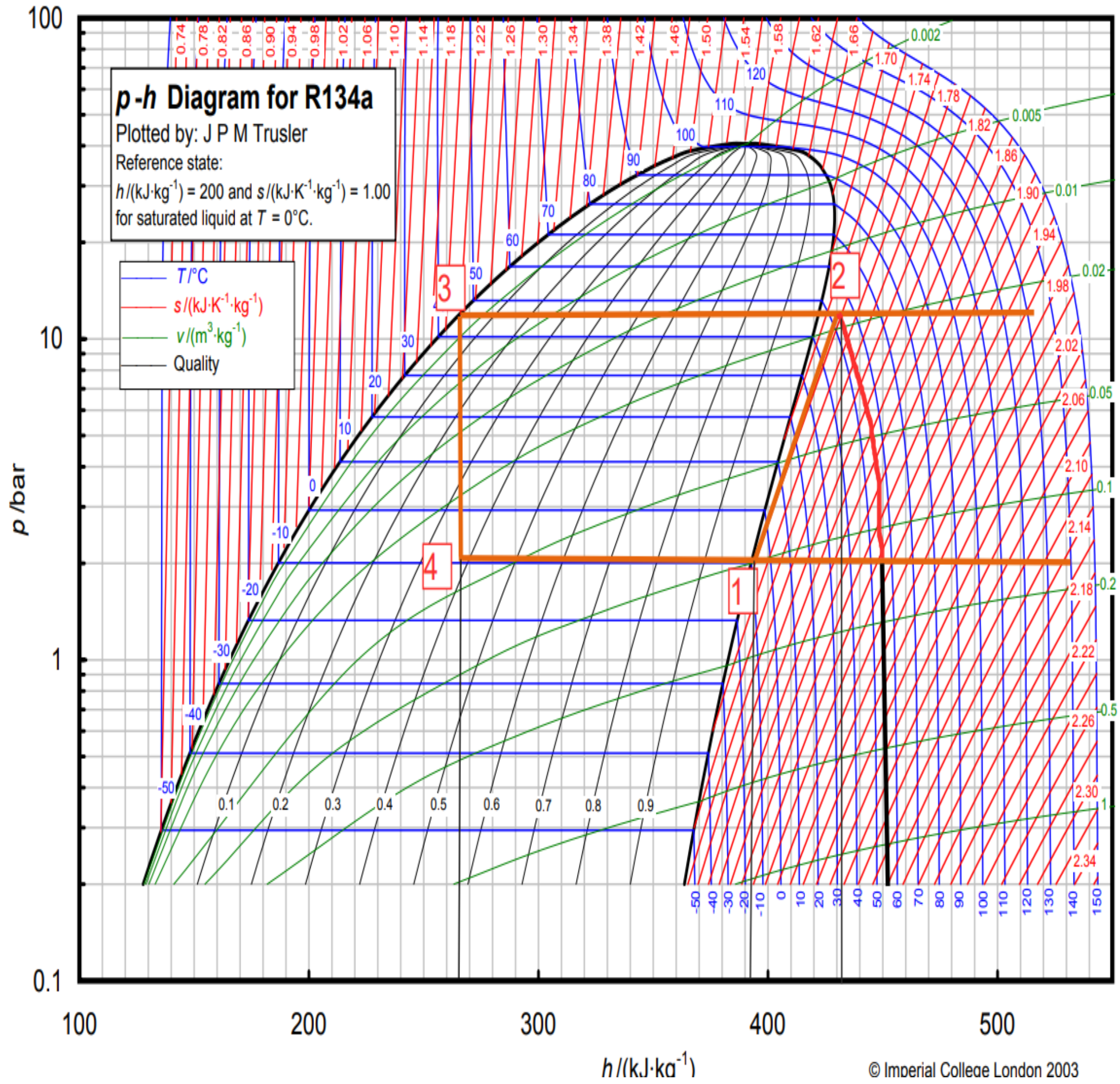

Fig 3.5: Plotting of design temperatures on P-h chart of R134a

Processes shown in the above chart are:

Process 1-2: Isentropic Compression

Process 2-3: Isobaric Heat Rejection in Condenser

Process 3-4: Throttling in Expansion valve (Capillary Tube)

Process 4-1: Isobaric Heat Addition in Evaporator

Enthalpies obtained from the above chart are:

Table 3.2: Enthalpies obtained after plotting design temperatures in P-h chart of R134a

h_1	392 kJ/kg
h_2	432 kJ/kg
h_3	266 kJ/kg
h_4	266 kJ/kg

3.4.2.3 Compressor's efficiencies

The overall compressor efficiency was obtained by calculating mechanical, volumetric and electrical efficiencies.

Volumetric efficiency $(\eta_v) = 1 + C - C\left(\frac{P_2}{P_1}\right)^{\frac{1}{\gamma}}$

Mechanical efficiency$(\eta_m) = \frac{Output\ Power}{Input\ Power}$

Electrical Efficiency $(\eta_e) = \frac{P_i}{P_c}$ = input power / rated power of the compressor

Overall Efficiency= $\eta_v * \eta_m * \eta_e$

3.4.2.3.1 Mechanical efficiency

Due to insufficient compressor data the mechanical efficiency was set to a typical Value of 0.90 obtained from relevant literature sources [10].

3.4.2.3.2 Volumetric efficiency

Following formulas were used to calculate the volumetric efficiency of the compressor

Specific heat capacity of R-134a at constant pressure is given by

$$C_p = C_{p1} + C_{p2}T + C_{p3}T^2 \quad [24, eq. (3.1)]$$

Specific heat capacity of R-134a at constant volume is given by

$$C_v = a + bT + cT^2 + dT^3 + \frac{f}{T^2} \quad [24, eq. (3.2)]$$

Heat Capacity Ratio of R-134a is given by

$$\gamma = \frac{C_p}{C_v} \quad [24, eq. (3.3)]$$

Clearance volume for the compressor is given by

$$Clearance\ volume\ (V_c) = clearance(c) \times stroke\ volume(v) \quad [3, eq. (3.4)]$$

Stroke Volume can be obtained from the Compressor data sheet. However, due to insufficient compressor data clearance was considered to be 4% from the relevant literature source [39].

Clearance ratio is given by

$$Clearance\ ratio\ (C) = \frac{Clearance\ volume\ (V_c)}{Stroke\ volume\ (v)} \quad [3, eq. (3.5)]$$

Volumetric efficiency of compressor is given by

$$\eta_v = 1 + C - C\left(\frac{P_2}{P_1}\right)^{\frac{1}{\gamma}} \quad [3, eq. (3.6)]$$

Here, $\frac{P_2}{P_1}$ is the pressure ratio and can be obtained from P-h chart

3.4.2.3.3 Electrical Efficiency

Electrical Power consumed (input power) by compressor is given by

$$Electrical\ power\ consumed(P_i) = Rated\ current \times voltage \quad [eq. (3.7)]$$

Electrical Efficiency is given by

$$\eta_e = \frac{P_o}{P_i} \qquad \text{eq. (3.9)}$$

Here output power of compressor (P_o) is the compressor rated power which can be obtained from the compressor data sheet.

3.4.2.5 Mass flow rate

Mass flow rate for the VCR system is given by

$$Compressor\ rated\ Power \times \eta_v \times \eta_e \times \eta_m = \dot{m}\ (h_2 - h_1) \qquad \text{[3, eq. (3.10)]}$$

3.4.2.6 Required Capacity

Required capacity for the evaporator is given by

$$Q_{evap} = \dot{m}\ (h_1 - h_4) \qquad \text{[3, eq. (3.10)]}$$

Required capacity for the condenser is given by

$$Q_{cond} = \dot{m}\ (h_2 - h_4) \qquad \text{[3, eq. (3.11)]}$$

3.4.3 Selection of Capillary Tube

The size of the capillary tube was selected from the capillary tube selection guide based on the evaporating temperature of our system and the rated cooling capacity of our compressor.

3.5 Procurement of Materials

All the above-mentioned components were purchased according to the calculated selection requirements. The remaining components like pipes and fittings were purchased in standard sizes typically used for the VCR system. The required fabricating tools like pipe cutter, flaring tools and brazing tools were also acquired.

3.6 Fabrication

The components were assembled, and the system was fabricated in accordance with the schematic design. Some modifications were incorporated that made the fabrication easier. The fabrication process primarily encompassed various pipe works like cutting, flaring, swaging, and brazing. These techniques were employed to connect different components through pipes, forming an integrated system.

3.7 Testing of Fabricated Unit

Once the fabrication of the unit was completed, the testing was carried out in Himal Refrigeration & Electrical Industries PVT. Ltd to check the leakages in the set-up.

3.7.1 Nitrogen flushing and soap bubble test

After the system assembly, the tubes were flushed with nitrogen, and the soap bubble test was conducted. The test revealed leakage in the system, and these leaks were corrected by re-brazing the joints with leakage and tightening the flare nuts. When these did not work the faulty components like flares and pressure gauge adaptors were changed.

3.7.2 Nitrogen Pressure Testing

The nitrogen gas was filled into the system at 130 psi, and the system was left undisturbed for 48 hours to ensure that the pressure held and there were no leakages following the soap bubble test.

3.7.3 Vacuuming

After the nitrogen pressure test, the nitrogen gas present in the tubes were vacuumed out with the vacuuming machine.

3.7.4 Refrigerant Charging

Before the refrigerant charging, the calculation of the nature of the working cycle was done which determined the required temperatures and enthalpy values. The volume of the tubes was measured from the fabricated system and multiplied by the densities of the refrigerant at different temperatures to get the mass of the refrigerant required [25].

Cylindrical pipe sizes: ¼ inches and ⅜ inches in diameters.

Cross-sectional Area(A): $\frac{\pi d^2}{4}$

Volume(V) = Cross-Sectional Area(A) * length of tubes(L)

Mass(m) = volume(V) * density(ρ)

3.8 System Operation

After a series of tests were conducted and it was verified that our set-up was free of leakages, refrigerant (R-134a) was charged into the system. Electrical connections of the compressor and fans of the evaporator and condenser were completed. The system was then operated.

3.9 Selection of Heat addition method

The finned tube heat exchanger was selected because it facilitated the heat addition process and its budget-friendly nature was advantageous. The heat addition method that worked best for the finned tube heat exchanger (forced type) was selected. The ability of the heating component to reach the required temperature for the experiment was also considered.

3.10 Experimentation

The experiment was conducted as per our project's objective. Pressure gauges and thermometers were placed in various places throughout the system through which the pressure and temperature at different states were obtained. Clamp meter was used to measure the current consumed by the compressor for the performance analysis.

3.11 Performance Analysis

3.11.1 COP

COP of the system is given by

$$COP = \frac{(h_1 - h_4)}{h_2 - h_1} \qquad [3, \text{eq. } (3.13)]$$

3.11.2 Percentage increase in COP

If COP_1 and COP_2 are the COPs of VCR before and after the addition of heat, then the percentage increase in COP can be calculated as

$$\%\, increase\ in\ COP = \frac{COP_2 - COP_1}{COP_1} \times 100 \qquad [15, \text{eq. } (3.14)]$$

3.11.3 Power required to run Compressor

Let P_1 and P_2 be the power required to run the compressor before and after the addition of heat, then it can be calculated as

$$P_1 = \frac{\dot{m}\,(h_1 - h_4)}{60 \times COP_1} \qquad [15, eq. (3.15)]$$

$$P_2 = \frac{\dot{m}\,(h_{1new} - h_{4new})}{60 \times COP_2} \qquad [15, eq. (3.16)]$$

3.11.4 Percentage reduction in Power to run Compressor

Let P_1 and P_2 be the power required to run the compressor before and after the addition of Solar Thermal respectively, then percentage reduction in power required to run the compressor is given by

$$\%\,Reduction = \frac{P_1 - P_2}{P_1} \times 100 \qquad [15, eq. (3.17)]$$

3.12 Validation

At the end of the project, all the results obtained were validated by conducting thorough literature review and expert consultation.

3.13 Documentation

The documentation was completed by following the guidelines provided by the department.

CHAPTER FOUR: RESULTS AND DISCUSSION

4.1 Output

4.1.1 Selection of Compressor

The Siberian GFF66AA compressor having following specifications was selected.

Table 4.1: Compressor Specifications [26]

Type	Hermetic LBP
Refrigerant	R134a
Power	¼ HP
Evaporating Temperature Range	-35℃ to -10℃
Max Peak Condensing Temperature	70℃
Max Operating Discharge Temperature	120℃
Displacement	6.6 cc
Rated Voltage	220V-240V
Max Rated Current	0.92

Fig 4.1: Compressor

4.1.2 Selection of Evaporator and Condenser

The calculations for the selection requirements of the evaporator and condenser were done as follows:

From P-H chart of R134a enthalpies at different states were

h_1 = 392 kJ/kg

h_2 = 432 kJ/kg

h_3 = 266 kJ/kg

h_4 = 266 kJ/kg

For volumetric efficiency

Stroke Volume (v) = 6.6 cm^3

Clearance (c) = 4% [27]

$$Clearance\ volume\ (V_c) = clearance\ \times stroke\ volume$$

$$= 4\% \times 6.6$$

$= 0.264\ cm^3$

$Clearance\ \ ratio\ (C) = \frac{V_c}{v}$

$= 0.04$

From P-H Chart

Pressure ratio (P_1/P_2) = 1/6

$C_p = C_{p1} + C_{p2}T + C_{p3}T^2$

T = reference Temperature = 273 K

$C_{p1} = 1.94006\ E{+}01 \frac{J}{mole}.K$

$C_{p2} = 2.58531\ E{-}01\ \frac{J}{mole}.K$

$C_{p3} = = -1.29665\ E{-}04 \frac{J}{mole}.K$

$C_p = 82.69 \frac{J}{mole}.K$

For R-134a , 102.03 g/mole

$C_p = 0.810447\ kJ/(kg.K)$

For C_v

$C_v = a + bT + cT^2 + dT^3 + \frac{f}{T^2}$

a = 3.154856 E+00

b = –1.656054 E–02

c = 4.353378 E–05

d = –3.754497 E–08

f = –3.023189 E+04

$C_v = 0.7088kJ/(kg.K)$

$\gamma = \frac{C_p}{C_v} = 1.14$

Now

$\eta_v = 1 + C - C\left(\frac{P_2}{P_1}\right)^{\frac{1}{\gamma}}$

$\eta_v = 0.8474$

For electrical efficiency

Maximum Rated Current of compressor = 0.92A [28]

$Input\ Power(P_i) = Rated\ current \times voltage$

= 0.92× 220

= 202.4 W

Input Power (P_o) = 143 W

Now,

$\eta_e = \frac{P_i}{P_c}$

$\eta_e = 0.7065$

For mechanical efficiency

$\eta_n = 0.95$

$Power \times \eta_v \times \eta_e \times \eta_m = \dot{m}\ (h_2 - h_1)$

(1/4) ×0.7457×0.8474×0.7065×0.90 = $\dot{m}$ (432-392)

$\dot{m}$ = 0.002511 kg/s

For COP

$COP = \frac{h_1 - h_4}{h_2 - h_1}$

COP = 3.15

Required Evaporator capacity

$Q_{evap} = \dot{m}\ (h_1 - h_4)$

= 0.002511× (392-266)

$Q_{evap} = 316.386\, W$

Selected Evaporator Capacity

The evaporators available on the market were only of standard sizes. We initially chose one of them to see if it met our requirements.

Rated Capacity of selected evaporator = 1/3 hp

$Q_{evap(Sel)} = Rated\ Capacity \times \eta_v \times \eta_e \times\ \eta_m \times COP$

= (1/3)×0.7457×1000×0.8474×0.7065×0.90×3.15

$Q_{evap(Sel)} = 421.887\, W$

The capacity of the evaporator initially chosen came out to be *421.887* W which met our requirement of *316.386* W. So, this evaporator was selected. This evaporator is a finned tube evaporator with a fan set.

Fig 4.2: Evaporator

Required Condenser Capacity

$Q_{cond} =\ \dot{m}\ (h_2 - h_4)$

= 0.002511(432-266)

$Q_{cond} = 416.826\, W$

Selected Condenser Capacity

The condensers available on the market were only of standard sizes. We initially chose one of them to see if it met our requirements.

Rated Capacity of selected condenser= 1/3 hp

$$Q_{cond(Sel)} = Rated\ Capacity \times \eta_v \times \eta_e \times \eta_m \times \frac{h_2 - h_3}{h_2 - h_1}$$

$$= (⅓) \times 0.7457 \times 1000 \times 0.8474 \times 0.7065 \times 0.90 \times \frac{432-266}{432-392}$$

$$Q_{cond(Sel)} = 555.82W$$

The capacity of the condenser initially chosen came out to be 555.82W which met our requirement of 416.826W. So, this evaporator was selected. This condenser is a finned tube condenser with a fan set.

Fig 4.3: Condenser with fan set

4.1.3 Selection of Capillary Tube

The following selection guide was followed for the selection of the capillary tube. The rated cooling capacity of our compressor is 186.4W and our evaporating temperature is -10℃ so the capillary tube of 0.91 mm diameter and 3.3m length was selected [29].

4.1.4 Fabrication

The fabrication of the system resulted in the following setup.

Fig 4.4: Experimental Setup

4.1.5 Refrigerant Charging

Table 4.2: Refrigerant Charging Calculation Sheet

Copper Tube	Dia (inch)	Dia (mm)	Length of Pipe (mm)	Volume (m^3)	Temperature at the point (°C)	Density (ρ)	Mass of the Refrigerant required(kg)
Liquid Flow 1	0.25	6.35	533.4	1.68924E-05	-10	1327.4	0.022422972
Liquid Flow 2	0.375	9.525	1041.4	7.42059E-05	-10	1327.4	0.098500912
Liquid Flow 3 (condenser)	0.375	9.525	2413	0.000171941	-10	1327.4	0.228233821
Liquid Flow 4 (evaporator)	0.375	9.525	4597.4	0.000327592	-10	1327.4	0.43484549
Liquid Flow 5 (filter)	0.75	19.05	127	3.6198E-05	-10	1327.4	0.048049225

Vapour Flow 1	0.375	9.525	1676.4	0.000119453	+55	76.79	0.009172827
Vapour Flow 2	0.375	9.525	1828.8	0.000130313	+55	76.79	0.01000672
Vapour Flow 3	0.25	6.35	2667	8.4462E-05	+46	41.7604	0.003527167
Vapour Flow HX 1	0.375	9.525	4826	0.000343881	+46	41.7604	0.014360608
Vapour Flow HX 2	0.375	9.525	4826	0.000343881	+55	76.79	0.026406622
Vapour Flow (condenser)	0.375	9.525	2413	0.000171941	+46	41.7604	0.007180304
Vapour Flow (evaporator)	0.375	9.525	4597.4	0.000327592	+55	76.79	0.025155782
Total							0.927862451

The calculated value for the mass of refrigerant to be charged into the system was 0.927 kg.

4.2 Experimental Data

Once the system became operable, experiment was conducted to obtain necessary data

4.2.1 Data for heat addition before compressor

4.2.1.1 Normal operation mode

Ambient Temperature: 26°C

Table 4.3: Baseline data for heat addition before compressor

	Temperature (in °C)	Pressure (in kPa)	Current (A)
Compressor inlet	$T_1 = 26$	$P_1 = 140$	0.58
Compressor Outlet	$T_2 = 67.7$	$P_2 = 1100$	
Condenser inlet	$T_3 = 67.7$	$P_3 = 1080$	
Condenser Outlet/capillary tube inlet	$T_4 = 27.2$	$P_4 = 1080$	
Evaporator inlet/ capillary tube outlet	$T_5 = -15.6$	$P_5 = 180$	
Evaporator outlet	$T_6 = 23.2$	$P_6 = 160$	

4.2.1.2 Heat addition before compressor

Ambient Temperature: 26°C

Table 4.4: Pressure (in kPa) Data for heat addition before compressor

Position		Refrigerant Superheated by						
		3 °C	4 °C	5 °C	7 °C	8 °C	9 °C	10 °C
Compressor inlet	P_1	120	110	120	120	120	120	130
Compressor outlet	P_2	1000	870	1000	1020	1020	1030	1040
Condenser inlet	P_3	960	830	970	1000	1000	1000	1020
Condenser Outlet/capillary tube inlet	P_4	980	850	980	1000	1000	1020	1040
Evaporator inlet/ capillary tube outlet	P_5	160	140	170	180	180	180	180
Evaporator outlet	P_6	160	140	170	180	180	180	180

Table 4.5: Temperature (in °C) Data for heat addition before compressor

Position		Refrigerant Superheated by						
		3 °C	4 °C	5 °C	7 °C	8 °C	9 °C	10 °C
Compressor inlet	T_1	29	30	31	33	34	35	36
Compressor outlet	T_2	66.1	66	66.4	67.9	67.9	68.2	67.9
Condenser inlet	T_3	66.1	66	66.4	67.9	67.9	68.2	67.7
Condenser Outlet/capillary tube inlet	T_4	26.9	27	27.2	27.5	27.5	27.5	27.4
Evaporator inlet/ capillary tube outlet	T_5	-15.6	-15.6	-14.13	-12.73	-12.73	-12.7	-12.7
Evaporator outlet	T_6	23.9	23.9	23.9	23.9	23.9	23.9	23.7

4.2.2 Data for heat addition after compressor

4.2.2.1 Normal operation mode

Ambient Temperature: 17°C

Table 4.6: Baseline data for heat addition after compressor

	Temperature (in °C)	Pressure (in kPa)	Current (A)
Compressor inlet	$T_1 = 27.3$	$P_1 = 100$	0.46
Compressor Outlet	$T_2 = 58.9$	$P_2 = 820$	
Condenser inlet	$T_3 = 58.9$	$P_3 = 800$	
Condenser Outlet/capillary tube inlet	$T_4 = 19$	$P_4 = 820$	

Evaporator inlet/ capillary tube outlet	T_5 = -23	P_5 = 110	
Evaporator outlet	T_6 = 16.3	P_6 = 110	

4.2.2.2 Heat addition after compressor

Ambient Temperature: 17°C

Table 4.7: Pressure (in kPa) Data for heat addition after compressor

Position		Refrigerant Superheated by					
		0.6 °C	3.1 °C	4.1 °C	5.2 °C	7.1 °C	9.2 °C
Compressor inlet	P_1	140	140	140	150	150	160
Compressor outlet	P_2	980	1000	1000	1000	1000	1010
Condenser inlet	P_3	960	970	980	980	980	990
Condenser Outlet/capillary tube inlet	P_4	970	980	1000	1000	1000	1000
Evaporator inlet/ capillary tube outlet	P_5	180	180	180	180	180	180
Evaporator outlet	P_6	170	180	180	180	180	180

Table 4.8: Temperature (in °C) Data for heat addition before compressor

Position		Refrigerant Superheated by					
		0.6 °C	3.1 °C	4.1 °C	5.2 °C	7.1 °C	9.2 °C
Compressor inlet	T_1	21.6	21.6	21.5	21.5	21.4	21.3
Compressor outlet	T_2	59.2	59.8	60	60.2	60.3	60.3
Condenser inlet	T_3	59.5	62	64.1	66	68.1	70
Condenser Outlet/capillary tube inlet	T_4	20	20.4	20.4	20.4	20.4	20.4

Evaporator inlet/ capillary tube outlet	T_5	-12.6	-12.3	-12	-11.9	-11.9	-11.7
Evaporator outlet	T_6	14.3	14.4	14.4	14.4	14.4	14.3

4.3. Results of heat addition before compressor

4.3.1 Normal Operation

Table 4.9: Result of baseline cycle of heat addition before compressor

h1 (enthalpy at compressor inlet)	276.5
h2 (enthalpy at compressor outlet)	299.8
h5 (enthalpy at evaporator inlet)	89.55
h6 (enthalpy at evaporator outlet)	273.3
v1 (specific volume at compressor inlet)	0.1692
Refrigerating Effect	183.75
Work done (kJ/kg)	23.3
COP	7.907
Current	0.58

4.3.2 Heat addition before compressor

Table 4.10: Result of heat addition before compressor

Temperature at compressor inlet	**29**	**30**	**31**	**33**	**34**	**35**	**36**
h1 (enthalpy at compressor inlet)	279.5	280.3	281.2	283	283.7	284.7	285.1
h2 (enthalpy at compressor outlet)	299.8	299.7	300.1	301.3	301.3	301.5	301
h5 (enthalpy at evaporator inlet)	89.12	89.26	89.55	89.98	89.98	89.98	89.83

h6 (enthalpy at evaporator outlet)	274.3	274.3	274.1	274	274	274	273.8
v1 (specific volume at compressor inlet)	0.2004	0.2011	0.2019	0.2034	0.204	0.2047	0.2051
Refrigerating Effect	185.18	185.04	185.04	184.02	184.02	184.02	183.97
Work done (kJ/kg)	20.3	19.4	18.9	18.3	17.6	16.8	15.9
COP	9.116	9.563	9.763	10.056	10.43	10.92	11.55
Current	0.55	0.54	0.54	0.53	0.52	0.51	0.51

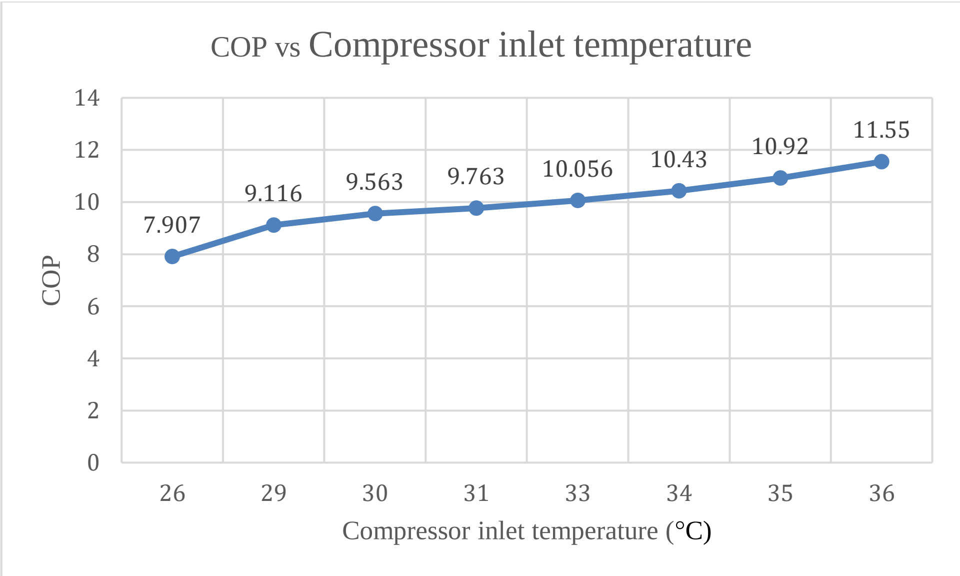

Fig 4.5: Variation of COP with increase in compressor inlet temperature

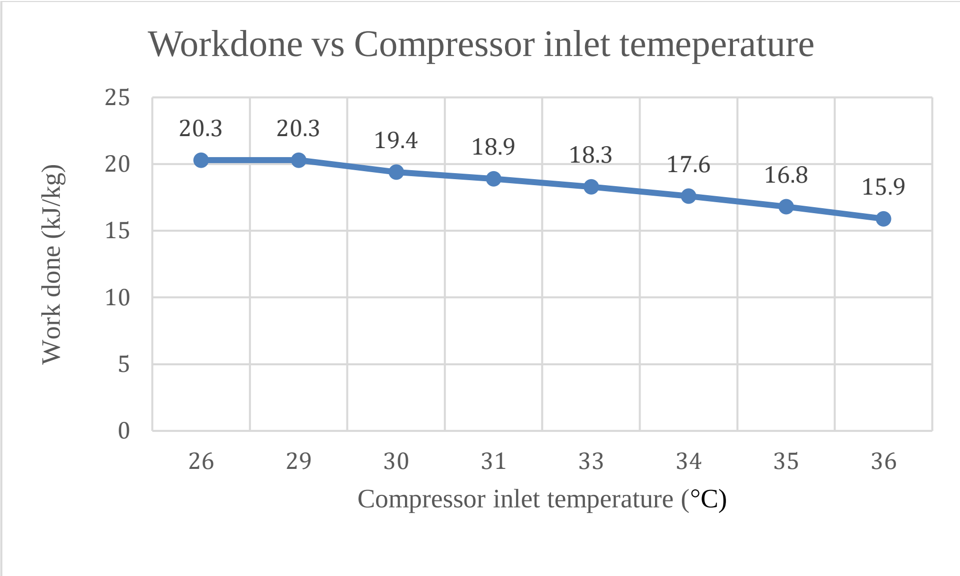

Fig 4.6: Variation of work done with increase in compressor inlet temperature

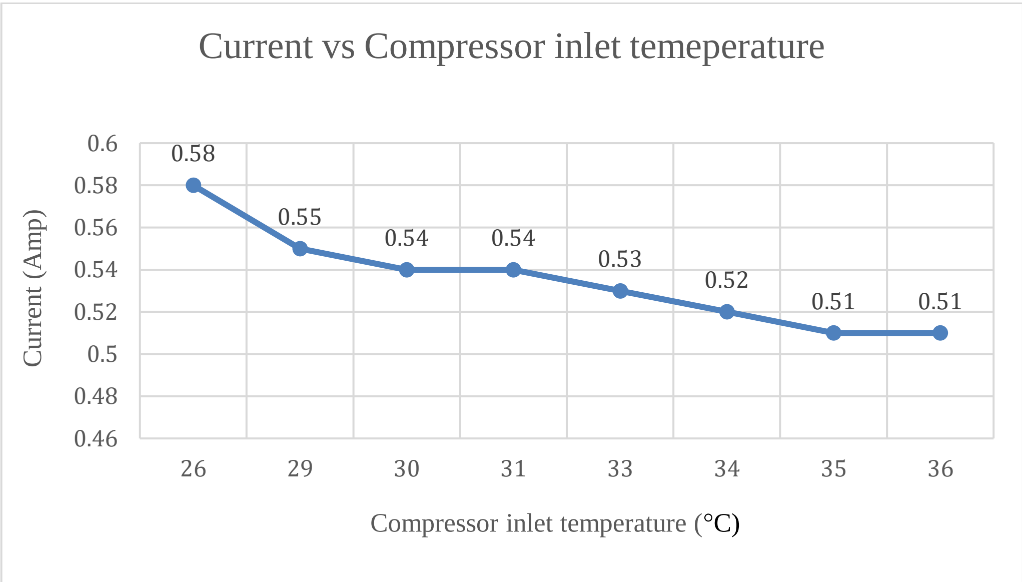

Fig 4.7: Variation of current with increase in compressor inlet temperature

The temperature of the refrigerant was increased from 26°C to 36°C at the inlet of the compressor. Enthalpy values at different states of the system were determined using EES software based on the obtained data. The refrigerating effect didn't show very significant variation while the work done per unit mass of refrigerant decreased progressively from 20.3 to 15.9 kJ/kg with the rising temperature. As a result, the COP of the system increased from 7.907 at the normal operating condition to 11.55 at 36°C experimental condition.

This result implies that addition of heat to the refrigerant before the compression process in the VCR system leads to an increase in the system's Coefficient of Performance (COP). This is consistent with the results obtained in the experiment conducted with solar powered AC syetem[30].

4.4 Results of heat addition after compressor

4.4.1 Normal Operation

Table 4.11: Result of baseline cycle of heat addition after compressor

h1 (enthalpy at compressor inlet)	279.5
h2 (enthalpy at compressor outlet)	299.8
h5 (enthalpy at evaporator inlet)	89.12
h6 (enthalpy at evaporator outlet)	274.3
v1 (specific volume at compressor inlet)	0.24
Refrigerating Effect	190.96
Work done (kJ/kg)	17
COP	11.23
Current	0.46

4.4.2 Result of heat addition after compressor

Table 4.12: Result of heat addition after compressor

Temperature at condenser inlet	**59.5**	**62**	**64.1**	**66**	**68.1**	**70**
h1 (enthalpy at compressor inlet)	272.7	272.7	272.7	272.5	272.4	272.1
h2 (enthalpy at compressor outlet)	292.9	293.2	293.4	293.6	293.7	293.5
h5 (enthalpy at evaporator inlet)	79.36	79.92	79.92	79.92	79.92	79.92
h6 (enthalpy at evaporator outlet)	265.9	265.8	265.8	265.8	265.8	265.7

v1 (specific volume at compressor inlet)	0.1664	0.1664	0.1664	0.1549	0.1549	0.1448
Refrigerating Effect	186.54	185.88	185.88	185.88	185.88	185.78
Work done (kJ/kg)	20.2	20.5	20.7	21.1	21.3	21.4
COP	9.23	9.07	8.98	8.81	8.73	8.68
Current	0.59	0.59	0.6	0.6	0.6	0.61

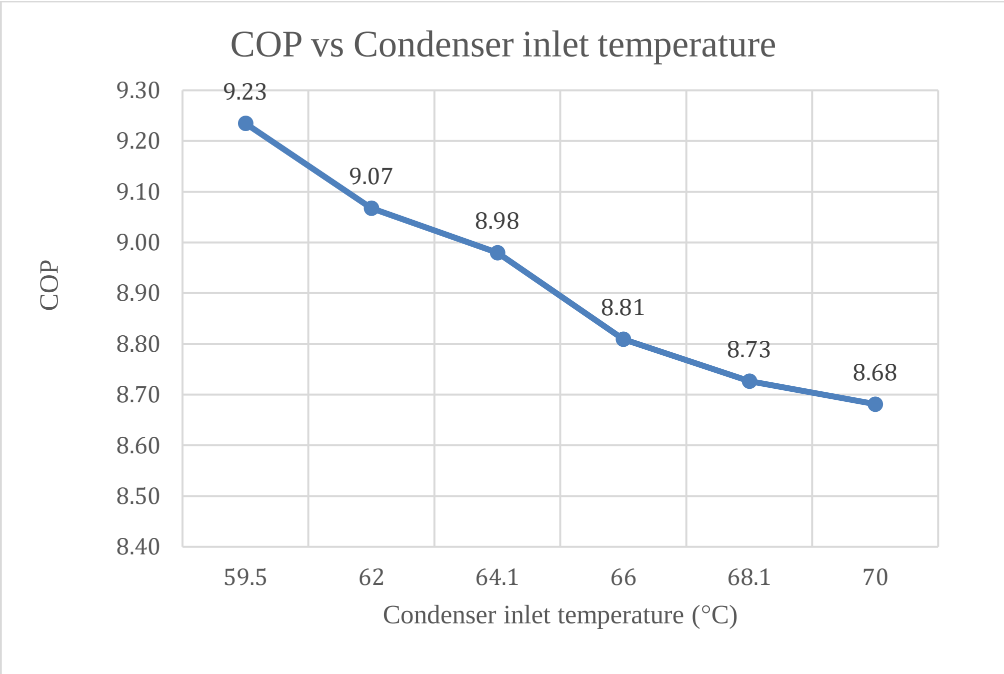

Fig 4.8: Variation of COP with increase in condenser inlet temperature

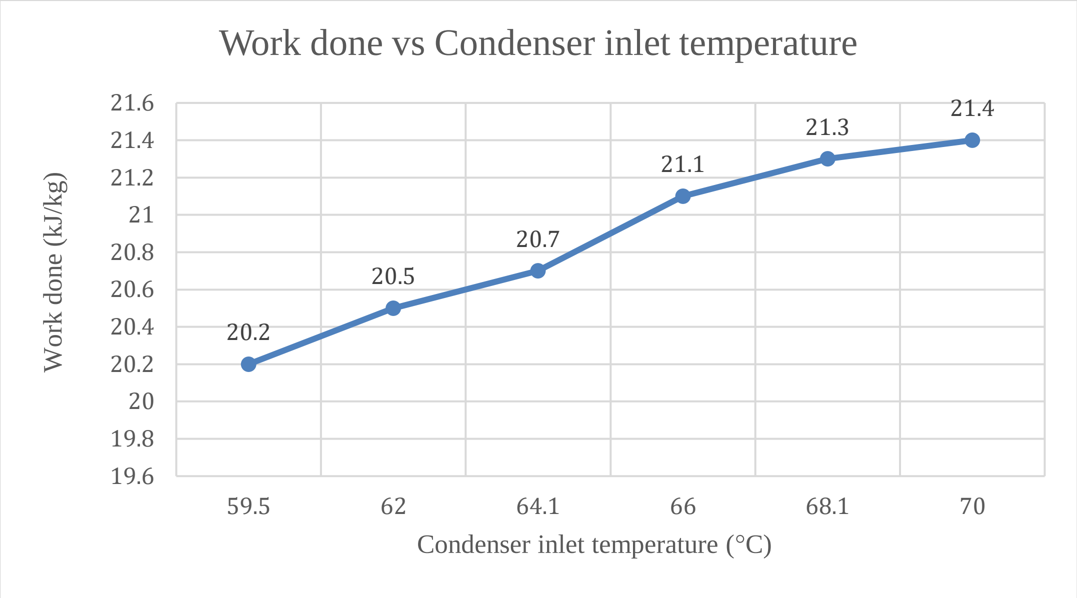

Fig 4.9: Variation of work done with increase in condenser inlet temperature

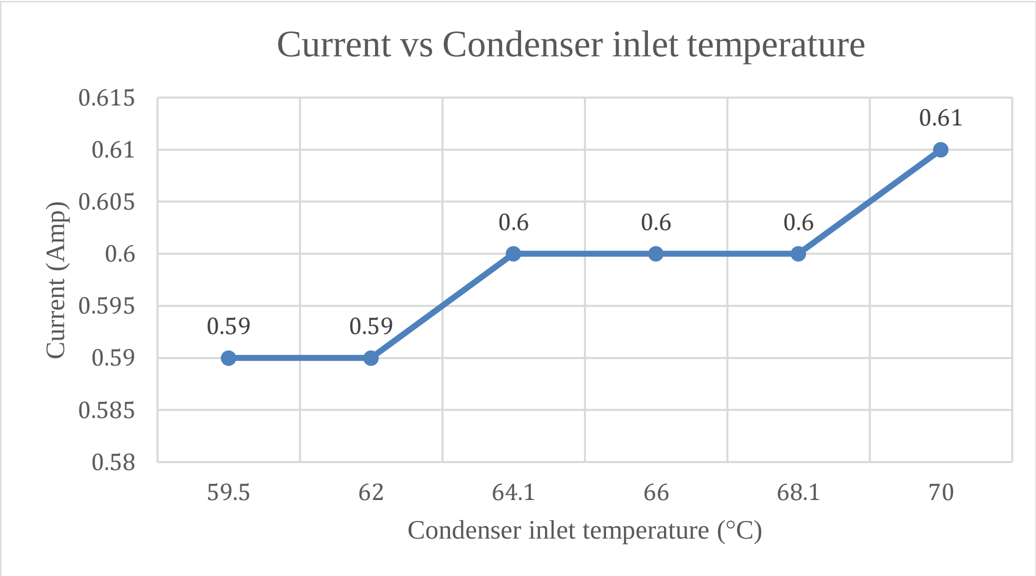

Fig 4.10: Variation of current with increase in condenser inlet temperature

The refrigerant was heated after the compression process increasing the condenser inlet temperature from 59.5°C to 70°C. Enthalpy values at various points in the system were calculated using the EES software. The analysis of the provided data indicated minimal fluctuation in the refrigerating effect, remaining around 185.88 kJ/kg. Concurrently, the specific work input (W) increased from 20.2 to 21.4 kJ/kg. Consequently, there was a decline in the Coefficient of Performance (COP) from 9.234 to 8.68 with the rising temperature. Meanwhile, the electrical current drawn by the compressor showed a minor increment from 0.59 to 0.61 A, which signifies an increase in power consumption of the compressor to maintain the same refrigerating effect.

The results suggest that adding heat to the refrigerant after the compressor in the VCR system leads to a decrease in the system's Coefficient of Performance (COP) due to increase in condenser temperature. This finding aligns with previous experimental results reported by [31].

4.5 Comparison of P-h chart

4.5.1 Baseline cycle and cycle of heat addition before compressor

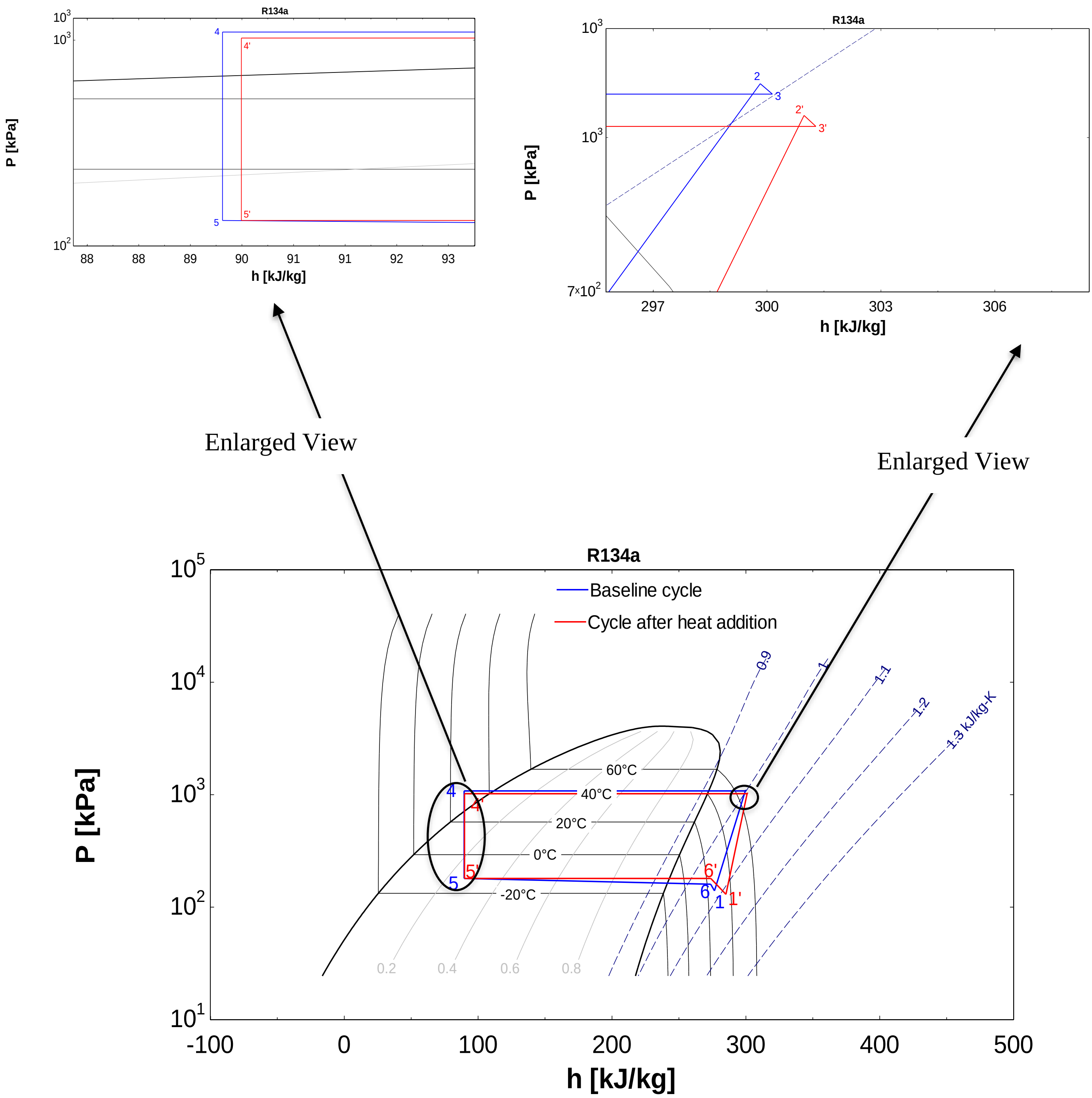

Fig 4.11:Comparison of P-h diagram of heat addition before compressor and baseline cycle

Fig: 4.11 is the comparison of P-h diagram of heat addition to the system before the compression process at 36^{o}C temperature at the compression inlet with the baseline cycle. The blue line represents the baseline cycle while the red line represents the cycle after heat addition. The line 6’-1’ represents the heat addition process before the compressor.

The pressure seems to have decreased during the heat addition process, likely due to a pressure drop in the heat exchanger tube. Comparing the lines 1’-2’ and 1-2 on the graph, we observe that the compression process after heat addition (1’-2’) is steeper. This indicates a smaller enthalpy difference between the compressor outlet and inlet in the cycle following heat addition, signifying a reduction in the work done for this cycle.

4.5.2 Baseline cycle and cycle of heat addition after compressor

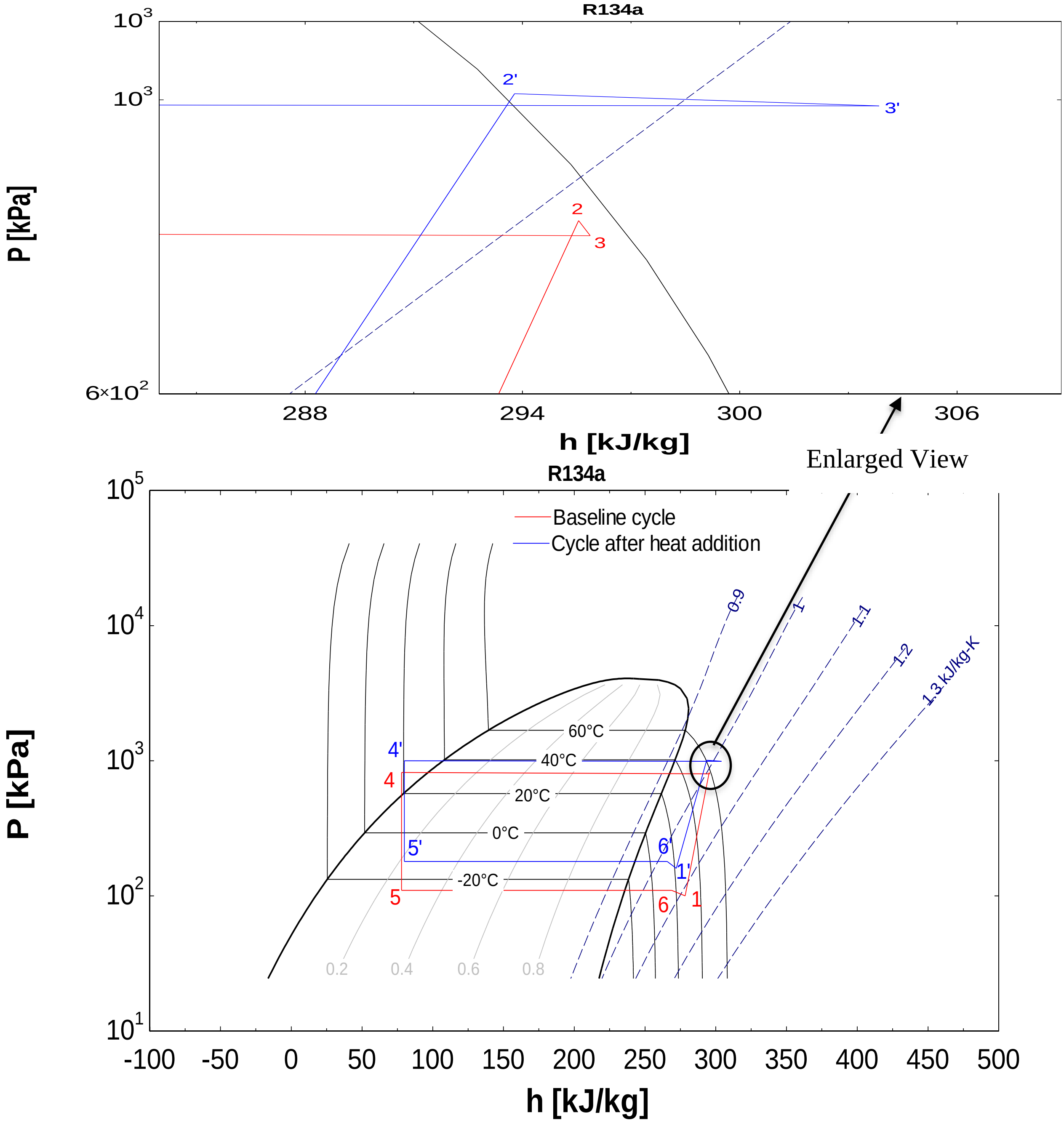

Fig 4.12: Comparison of P-h diagram of heat addition after compressor and baseline cycle

Fig: 4.12 is the comparison of P-h diagram of heat addition to the system after the compression process at 70^{o}C temperature at the condenser inlet with the baseline cycle. The red line represents the baseline cycle while the blue line represents the cycle after heat addition. The line 2’-3’ represents the heat addition process before the compressor. The pressure seems to have decreased during the heat addition process, likely due to a pressure drop in the heat exchanger tube. Comparing the lines 1’-2’ and 1-2 on the graph, we observe that the compression process after heat addition (1’-2’) is more slanted. This indicates a greater enthalpy difference between the compressor outlet and inlet in the cycle after heat addition, signifying an increase in the work done for this cycle.

4.6 Comparison of T-s diagram

4.6.1Baseline cycle and cycle after heat addition before compressor

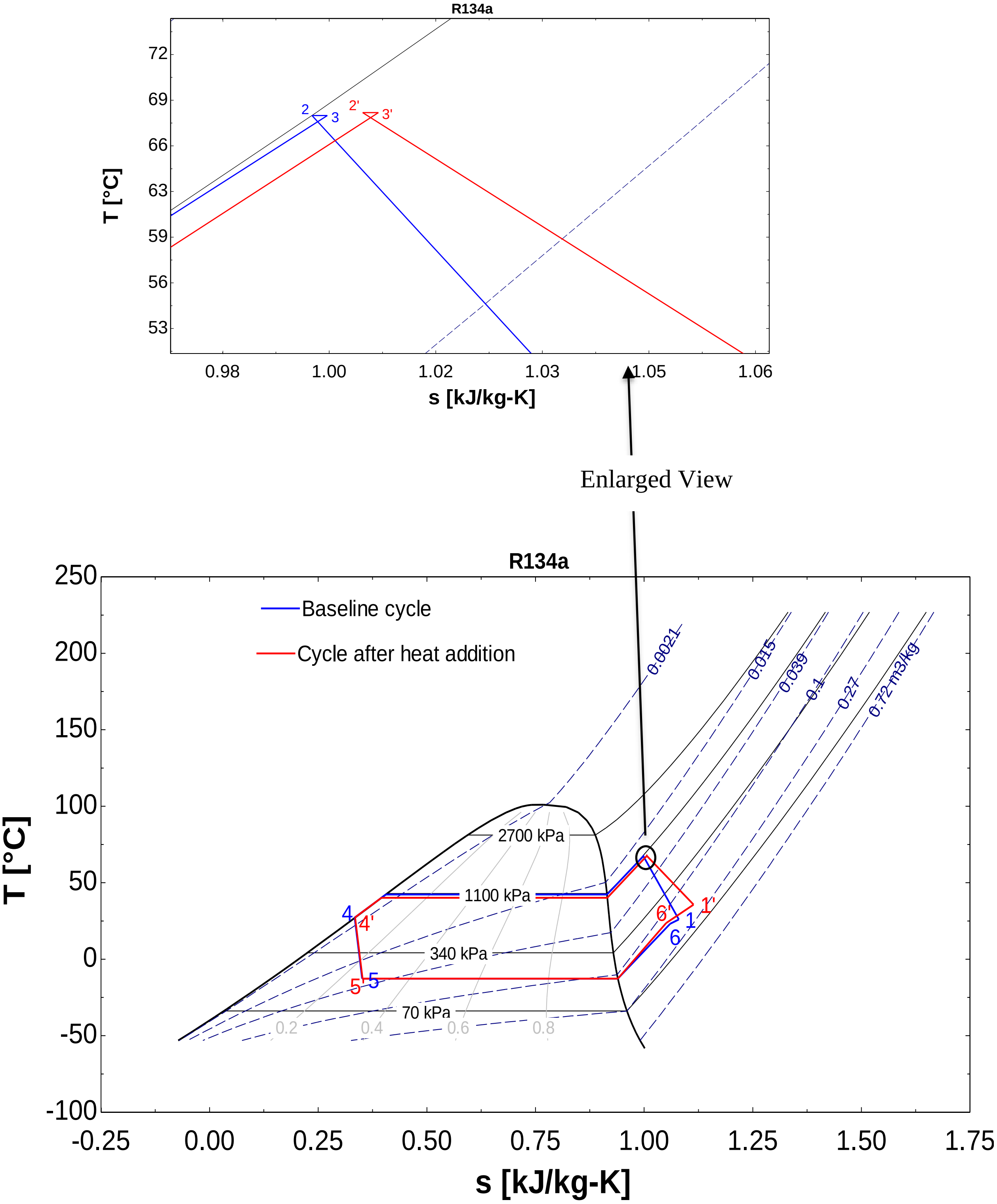

Fig 4.13: Comparison of T-s diagram of heat addition before compressor and baseline cycle

Fig: 4.13 is the comparison of T-s diagram of heat addition to the system before the compression process at 36^{o}C temperature at the compression inlet with the baseline cycle. The blue line represents the baseline cycle while the red line represents the cycle after heat addition. The line 6’-1’ represents the heat addition process before the compressor increasing temperature in the diagram. In this diagram, it is evident that the compression process following heat addition, depicted by line 1’-2’, tends more towards isothermal compression compared to the baseline cycle.

4.6.2 Baseline cycle and cycle after heat addition after compressor

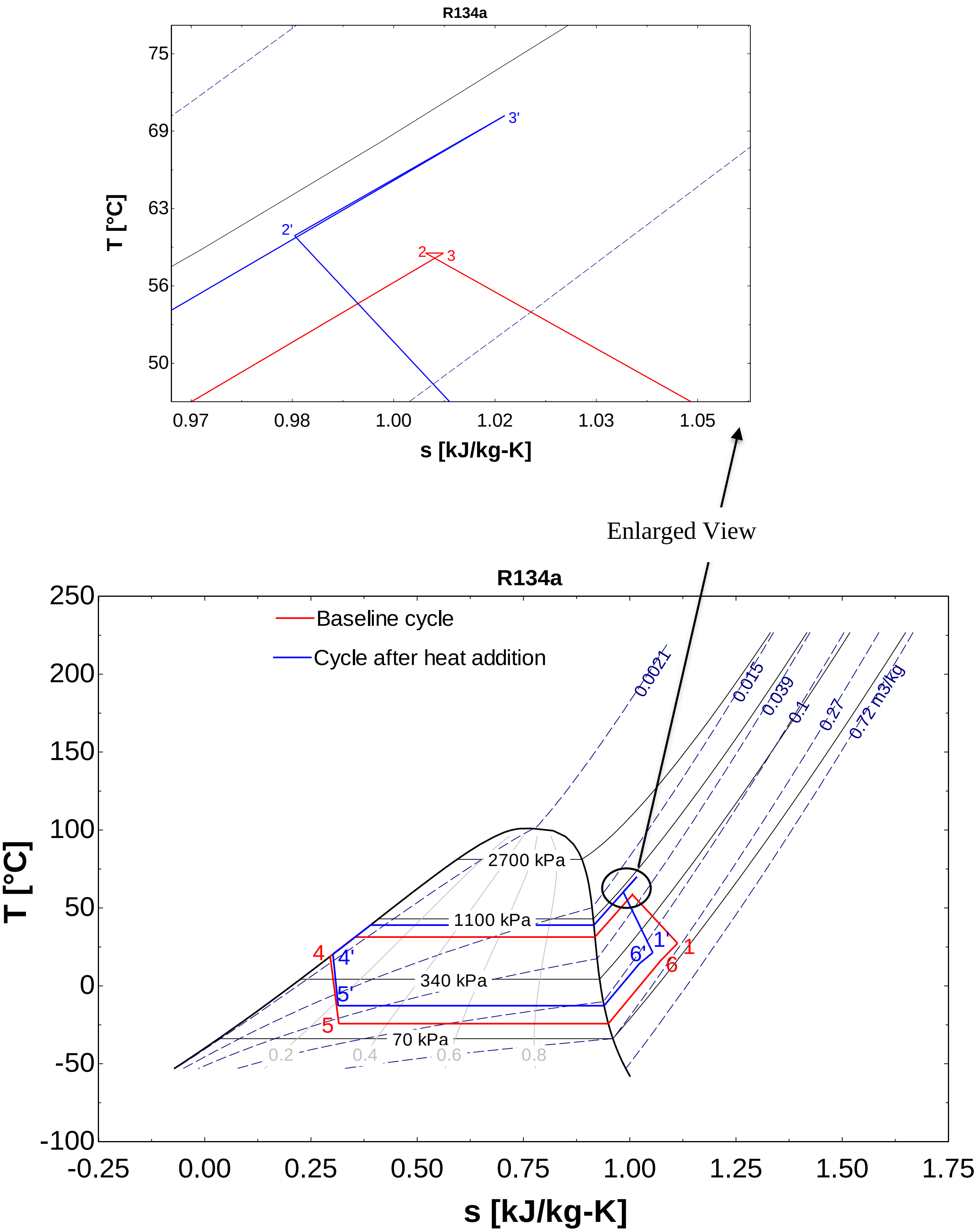

Fig 4.14: Comparison of T-s diagram of heat addition after compressor and baseline cycle

Fig: 4.14 is the comparison of T-s diagram of heat addition to the system after the compression process at 70^{o}C temperature at the condenser inlet with the baseline cycle. The red line represents the baseline cycle while the blue line represents the cycle after heat addition. The line 2’-3’ represents the heat addition process before the compressor which can be seen by increasing temperature in the diagram. In this diagram, it is evident that the compression process following heat addition, depicted by line 1’-2’, tends less towards isothermal compression compared to the baseline cycle.

4.7 Limitations

Limitations of this projects are:

i. Variations in experimental conditions, such as deviation in ambient temperature from the intended design condition, could have potentially impacted the obtained experimental data.

ii. The obtained data may have some inaccuracies as the thermometers that were used had very slow response time and more accurate ones were limited by budget constraints.

4.8 Problems Faced

The challenges that we encountered while carrying out our project were:

i. The evaporators and condensers available in the market weren’t in the exact size that we required so these components were oversized in our system.

ii. The pressure gauge adaptors were found to be defective, resulting in persistent leaks and requiring extensive time and effort for rectification.

iii. The recurrent choking of the capillary tube prevented us from operating the system and conducting numerous experiments.

iv. The relay of the compressor kept failing due to capillary choking and required frequent replacement.

4.9 Budget Analysis

Table 4.13: Budget analysis

Components	**Quantity**	**Rate**	**Amount**
Compressor	1	8500	8500
Condenser and fan set	1	3500	3500
Evaporator and fan set	1	3500	3500
Heat exchanger and fan set	2	3500	7000
filter	1	100	100
capillary	20 ft	450	450
⅜ Elbow	15	130	1950
⅜ flare nut	15	90	1350
¼ flare nut	20	75	1500
¼ copper tee	8	110	880
⅜ copper tee	8	130	1040
¼ copper pipe	10 ft	60 /ft	600
⅜ copper pipe	10 ft	95 /ft	950
⅜ valve	3	800	2400
¼ valve	6	550	3300
Brazing tool set	1	2500	2500
Pressure gauge set	6	675	4050

Temperature gauge	6	500	3000
Refrigerant	1kg		1600
Heat Adding Component	1	3000	3000
Miscellaneous			5750
Total			**NPR 56920**

CHAPTER FIVE: CONCLUSION AND FUTURE ENHANCEMENT

5.1 Conclusion

The project concluded with the fabrication of a vapour compression refrigeration system, followed by a performance analysis. This analysis involved evaluating the system's efficiency by introducing heat before and after the compressor to the refrigerant R134a. The heat addition before compressor was conducted at ambient temperature of 26°C whereas the heat addition after compressor was conducted at 17°C ambient temperature. Adding heat before the compressor has shown significant improvement in the system performance. Increasing the superheat degree by 10 °C has resulted in increment of COP by 46.07% and decrement in current consumption of compressor by 12.07%. On the other hand, system's performance was degraded considerably when heat was added after the compressor. COP was decreased by 22.7% and current consumption of compressor was increased by 32.6%.

Superheating at compressor inlet can make vapour compression refrigeration system more energy efficient, which is extremely beneficial for the future where energy crisis may pose significant impact.

5.2 Scope for Future Enhancement

This experimental study conducted on the VCR system offers following potential avenues for further research and enhancements:

i. Future endeavours could involve conducting experiments during peak summer conditions to explore the system's performance further and gather additional valuable data.
ii. Upgrading the experimental setup with advanced instrumentation such as thermocouple thermometers for temperature measurement would enhance data accuracy and analysis capabilities.
iii. For enhanced data quality, the experiment can be conducted under more controlled environmental conditions and with a refined setup.
iv. Additionally, conducting the experiment in diverse locations and with various new refrigerants would provide insights into the performance of the system

under different ambient temperature and humidity conditions, as well as with different upcoming refrigerants

REFERENCES

[1] G. C. Briley, "A History of Refrigeration," *ASHRAE Journal*, 2004.

[2] S. K. Wang, *Handbook of Air Conditioning and Refrigeration*, 2nd ed. McGraw-Hill, 2001.

[3] R. S. Khurmi and J. K. Gupta, "Textbook of refrigeration and air conditioning," 2020.

[4] Mohd. K. Khan, R. Kumar, and P. K. Sahoo, "Flow characteristics of refrigerants flowing through capillary tubes – A review," *Applied Thermal Engineering*, vol. 29, no. 8–9, pp. 1426–1439, Jun. 2009, doi: 10.1016/j.applthermaleng.2008.08.020.

[5] M. Cuce and A. Pinar, "Innovative heating, cooling and ventilation technologies for low-carbon buildings," SciSpace - Paper, Jan. 2016, [Online]. Available: https://typeset.io/papers/innovative-heating-cooling-and-ventilation-technologies-for-2nz52kxnrv (accessed May 15, 2023).

[6] Y. Monschauer, C. Delmastro, and R. Martinez-Gordon, "Global heat pump sales continue double-digit growth," IEA, Mar. 31, 2023. [Online]. Available: https://www.iea.org/commentaries/global-heat-pump-sales-continue-double-digit-growth (accessed May 15, 2023).Available: https://www.iea.org/commentaries/global-heat-pump-sales-continue-double-digit-growth (accessed May 15, 2023).

[7] "Cooling - IEA," IEA. https://www.iea.org/energy-system/buildings/space-cooling https://www.iea.org/reports/the-future-of-heat-pumps/how-a-heat-pump-works (accessed May 16, 2023)."Cooling - IEA," IEA. https://www.iea.org/energy-system/buildings/space-cooling https://www.iea.org/reports/the-future-of-heat-pumps/how-a-heat-pump-works (accessed May 16, 2023).

[8] A. Aliyarzadeh, "COP Calculation and Monitoring in HVAC Application," Schneider Electric Blog, 2016. [Online]. Available: https://blog.se.com/industry/machine-and-process-management/2016/04/13/cop-calculation-monitoring-hvac-application/ (accessed May 16, 2023).

[9] S. Anand, A. Gupta, and S. K. Tyagi, “Simulation studies of refrigeration cycles: A review,” *Renewable & Sustainable Energy Reviews*, vol. 17, pp. 260–277, Jan. 2013, doi: 10.1016/j.rser.2012.09.021.

[10] J. U. Ahamed, R. Saidur, and H. H. Masjuki, “A review on exergy analysis of vapor compression refrigeration system,” *Renewable & Sustainable Energy Reviews*, vol. 15, no. 3, pp. 1593–1600, Apr. 2011, doi: 10.1016/j.rser.2010.11.039.

[11] İ. Karaçayli and E. Şimşek, “Exergetic investigation of the effects of superheating and subcooling on performance of a vapor compression refrigeration cycle,” *European Mechanical Science*, vol. 4, no. 4, pp. 152–157, Dec. 2020, doi: 10.26701/ems.742973.

[12] A. Maurizio, G. G. Cerri, and D. F. Eduardo, “Power reduction in vapour compression cooling cycles by power regeneration,” Energy Procedia, vol. 81, pp. 1184–1197, Dec. 2015, doi: 10.1016/j.egypro.2015.12.148.

[13] M. J. Bergander, “New regenerative cycle for vapor compression refrigeration,” Aug. 2005. doi: 10.2172/850491.

[14] A. A. Eidan, M. J. Alshukri, M. Al-Fahham, A. AlSahlani, and D. M. Abdulridha, “Optimizing the performance of the air conditioning system using an innovative heat pipe heat exchanger,” Case Studies in Thermal Engineering, vol. 26, p. 101075, Aug. 2021, doi: 10.1016/j.csite.2021.101075.

[15] M. Prasanna and P.S. Kishore, “Enhancement of COP in Vapour Compression Refrigeration System,” International Journal of Engineering Research & Technology (IJERT), vol. 3, no. 11, Art. no. 2278–0181, Nov. 2014.

[16] H. M. Alli et al., “Suction Line Heat Exchanger and its Impact on the Performance of the Vehicle Air Conditioning System at High Ambient Temperature,” International Journal of Applied Engineering Research, vol. 17, no. 6, Art. no. 0973–4562, 2022.

[17] M. N. Izham and T. M. I. Mahlia, “Effect of Ambient Temperature and Relative Humidity on COP of A Split Room Air Conditioner,” Journal of Energy & Environment, vol. 2, no. 1, pp. 35–38, 2010.

[18] M. Deymi-Dashtebayaz, M. Farahnak, M. Moraffa, A. Ghalami, and N. Mohammadi, “Experimental evaluation of refrigerant mass charge and ambient air temperature effects on performance of air-conditioning systems,” Heat and

Mass Transfer, vol. 54, no. 3, pp. 803–812, Oct. 2017, doi: 10.1007/s00231-017-2173-6.

[19] Y. Heredia-Aricapa, J. M. Belman-Flores, A. Mota-Babiloni, J. Serrano-Arellano, and J. J. G. Pabón, "Overview of low GWP mixtures for the replacement of HFC refrigerants: R134a, R404A and R410A," International Journal of Refrigeration, vol. 111, pp. 113–123, Mar. 2020, doi: 10.1016/j.ijrefrig.2019.11.012.

[20] Copper Development association Inc., Copper Tube Handbook Industry Standard Guide for the Design and Installation of Copper Piping Systems. CDA Publication.

[21] C. Migliaccio, Refrigerant Charging and Service Procedures for Air Conditioning, 1st ed. 2019.

[22] P. Bansal and G. Wang, "Numerical analysis of choked refrigerant flow in adiabatic capillary tubes," Applied Thermal Engineering, vol. 24, no. 5–6, pp. 851–863, Apr. 2004, doi: 10.1016/j.applthermaleng.2003.10.010.

[23] U. C. Rajmane, "Cascade Refrigeration System: R404A-R23 Refrigerant," Asian Journal of Managerial Science/Asian Journal of Managerial Science, vol. 6, no. 1, pp. 18–22, May 2017, doi: 10.51983/ajes-2017.6.1.1993.

[24] The Chemours Company FC, LLC. FreonTM, FreonTM 134a Thermodynamic Properties (SI Units). 2018.

[25] "Refrigerant R134a - properties." https://www.engineeringtoolbox.com/r134a-properties-d_1682.html (accessed May 12, 2023).

[26] Motech Refrigeration parts and equipments, GFF66AA Data Sheet.

[27] "Refrigeration & Air-Conditioning: Lesson 10. Reciprocating compressor-construction, working and maintenance." http://ecoursesonline.iasri.res.in/mod/page/view.php?id=98300 (accessed May 11, 2023).http://ecoursesonline.iasri.res.in/mod/page/view.php?id=98300 (accessed May 11, 2023).

[28] "refrigerator compressor, LBP, 1/6Hp, GFF44AA, GFF75AA, R134a, 220-240V~50Hz, RSIR, 130W , 0.65A, Cop: 1.31, Oil charge: 200ml, Compresseurs hermétiques Siberia - MBSM DOT PRO." https://www.mbsm.pro/46025.html?print=print (accessed May 11,

2023).https://www.mbsm.pro/46025.html?print=print (accessed May 11, 2023).

[29] Embraco Nidec, COMPRESSOR INSTALLATION INSTRUCTIONS. [Online]. Available: https://www.embraco.com (accessed May 11, 2023).

[30] A. Ö. Akyüz, R. Yıldırım, A. Güngör, and A. D. Tuncer, “Experimental investigation of a solar-assisted air conditioning system: Energy and life cycle climate performance analysis,” Thermal Science and Engineering Progress, vol. 43, p. 101960, Aug. 2023, doi: 10.1016/j.tsep.2023.101960.

[31] S. G. Kim and Kim, “Experiment and simulation on the performance of an autocascade refrigeration system using carbon dioxide as a refrigerant,” International Journal of Refrigeration, vol. 25, no. 8, pp. 1093–1101, Dec. 2002, doi: 10.1016/s0140-7007(01)00110-4.

ANNEX-A

EES Code for finding COP and plotting P-h diagram

```
$UnitSystem SI Mass KJ C KPa Rad

"Compressor inlet"

P [1] =160

T [1] =21.3

h [1] =enthalpy(R134a, P=P[1], T=T [1])

s[1] =entropy(R134a, P=P [1], T=T [1])

v [1] =Volume (R134a, T=T [1], P=P [1])

"compressor outlet"

P [2] =1020

T [2] =60.3

h [2] =enthalpy (R134a, P=P [2], T=T [2])

s [2] =entropy (R134a, P=P [2], T=T [2])

v [2] =Volume (R134a, T=T [2], P=P [2])

"condenser inlet"

P [3] =990

T [3] =70

h [3] =enthalpy (R134a, P=P [3], T=T [3])

s [3] =entropy (R134a, P=P [3], T=T [3])

v [3] = Volume (R134a, T=T [3], P=P [3])
```

"Condenser outlet"

P [4] =1000

T [4] =20.4

h [4] =enthalpy (R134a, P=P [4], T=T [4])

s [4] =entropy (R134a, P=P [4], T=T [4])

v [[4] =Volume (R134a, T=T [4], P=P [4])

"evaporator inlet"

P [5] =180

h [5] =h [4]

T [5] =Temperature (R134a, P=P [5], h=h [5])

s [5] =entropy (R134a, P=P [5], h=h [5])

v [5] =Volume (R134a, s=s [5], P=P [5])

"evaporator outlet"

P [6] =180

T [6] =14.3

h [6] =enthalpy (R134a, P=P [6], T=T [6])

s [6] =entropy (R134a, P=P [6], T=T [6])

v [6] =Volume (R134a, T=T [6], P=P [6])

P [7] =P [1]

T [7] =T [1]

```
h [7] =h [1]

v [7] =v [1]

s [7] =s [1]

COP = (h [6]-h [5])/ (h [2]-h [1])
```

EES Code for plotting T-s diagram

```
$UnitSystem SI Mass KJ C KPa Rad

"compressor inlet"

P[1]=100

T[1]=27.3

h[1]=enthalpy(R134a,P=P[1],T=T[1])

s[1]=entropy(R134a,P=P[1],T=T[1])

v[1]=Volume(R134a,T=T[1],P=P[1])


"compressor outlet"

P[2]=820

T[2]=58.9

h[2]=enthalpy(R134a,P=P[2],T=T[2])

s[2]=entropy(R134a,P=P[2],T=T[2])

v[2]=Volume(R134a,T=T[2],P=P[2])


"condenser inlet"
```

```
P[3]=800

T[3]=58.9

h[3]=enthalpy(R134a,P=P[3],T=T[3])

s[3]=entropy(R134a,P=P[3],T=T[3])

v[3]= Volume(R134a,T=T[3],P=P[3])


P[4]=800

x[4]=1

T[4]= Temperature(R134a,P=P[4],x=x[4])

h[4]=enthalpy(R134a,P=P[4],x=x[4])

s[4]=entropy(R134a,P=P[4],x=x[4])


P[5]=800

x[5]=0

h[5]=enthalpy(R134a,P=P[5],x=x[5])

s[5]=entropy(R134a,P=P[5],x=x[5])

v[5]=Volume(R134a,x=x[5],P=P[5])

T[5]= Temperature(R134a,P=P[5],x=x[5])


"condenser outlet"
```

```
P[6]=820

T[6]=19

h[6]=enthalpy(R134a,P=P[6],T=T[6])

s[6]=entropy(R134a,P=P[6],T=T[6])

v[6]=Volume(R134a,T=T[6],P=P[6])


"evaporator inlet"

P[7]=110

h[7]=h[6]

T[7]=Temperature(R134a,P=P[7],h=h[7])

s[7]=entropy(R134a,P=P[7],h=h[7])

v[7]=Volume(R134a,s=s[7],P=P[7])


P[8]=110

x[8]=1

T[8]=Temperature(R134a,P=P[8],x=x[8])

h[8]=enthalpy(R134a,P=P[8],x=x[8])

s[8]=entropy(R134a,P=P[8],x=x[8])

v[8]=Volume(R134a,x=x[8],P=P[8])
```

```
"evaporator outlet"

P[9]=110

T[9]=16.3

h[9]=enthalpy(R134a,P=P[9],T=T[9])

s[9]=entropy(R134a,P=P[9],T=T[9])

v[9]=Volume(R134a,T=T[9],P=P[9])


P[10]=P[1]

T[10]=T[1]

h[10]=h[1]

v[10]=v[1]

s[10]=s[1]
```

ANNEX-B

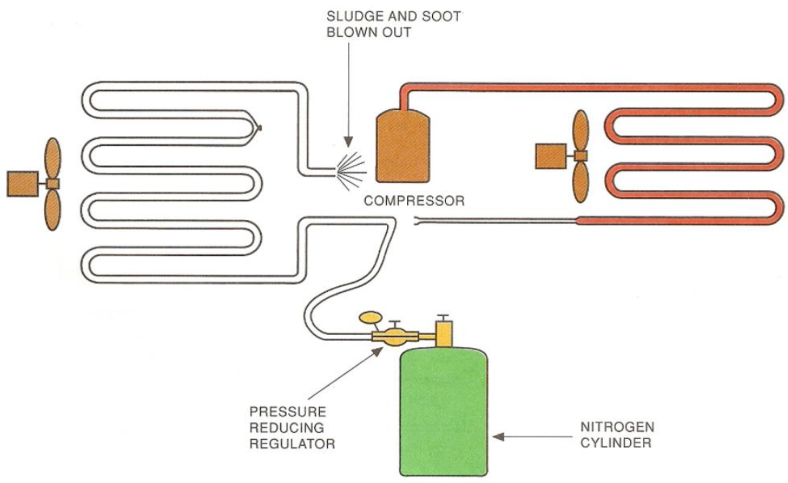

Fig: Nitrogen Flushing [24]

Fig: Bubble Testing

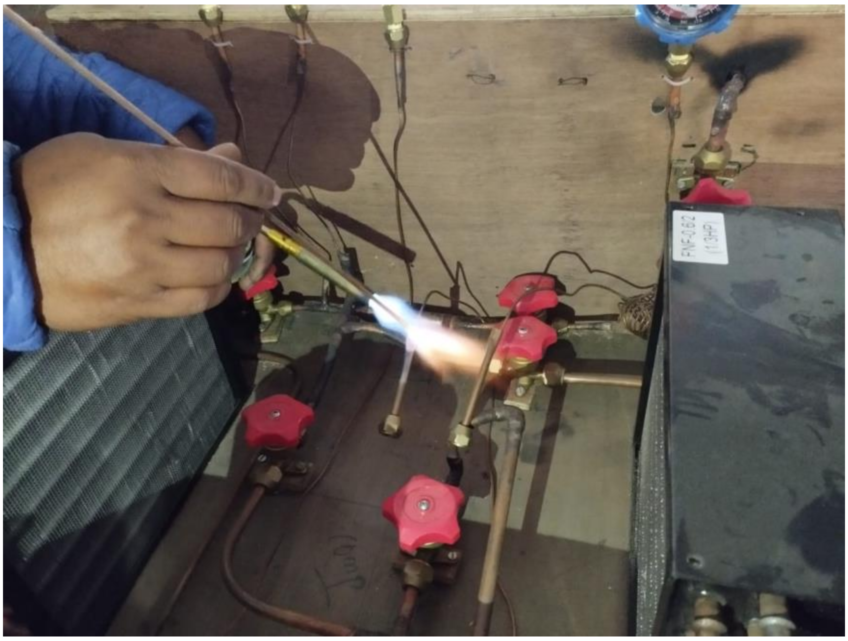

Fig: Brazing

Fig: Cutting copper pipe with tube cutter

Fig: Compressor

Fig : Evaporator

Fig : Condenser with fan set

Fig: fabricated system

Experimental Analysis on Vapour Compression Refrigeration System

ORIGINALITY REPORT

12%
SIMILARITY INDEX

PRIMARY SOURCES

1	elibrary.tucl.edu.np Internet	108 words — 1%
2	vibdoc.com Internet	64 words — 1%
3	www.methodstatementhq.com Internet	64 words — 1%
4	www.coursehero.com Internet	63 words — 1%
5	alamoashrae.org Internet	60 words — 1%
6	www.darshan.ac.in Internet	59 words — 1%
7	www.cram.com Internet	52 words — < 1%
8	docshare.tips Internet	50 words — < 1%
9	Bansal, P.K.. "Numerical analysis of choked refrigerant flow in adiabatic capillary tubes", Applied Thermal Engineering, 200404	45 words — < 1%

Crossref

10 c.coek.info
Internet
41 words — < 1%

11 vdoc.pub
Internet
38 words — < 1%

12 dte.karnataka.gov.in
Internet
36 words — < 1%

13 Tim Koopman, Tingting Zhu, Wilko Rohlfs. "Performance evaluation of air-source heat pump based on a pressure drop embedded model", Heliyon, 2024
Crossref
32 words — < 1%

14 Chen, Li-Chun. "Microstructure and Texture Development in Cold Rolled and Warm Plane-Strain Extruded Commercial Purity Aluminum", Drexel University, 2023
ProQuest
31 words — < 1%

15 huddleston.com.au
Internet
30 words — < 1%

16 www.homedepot.com
Internet
29 words — < 1%

17 Hadi Ghaebi, Amin Shekari Namin, Hadi Rostamzadeh. "Performance assessment and optimization of a novel multi-generation system from thermodynamic and thermoeconomic viewpoints", Energy Conversion and Management, 2018
Crossref
28 words — < 1%

18 Oliver, Jason Ryan. "A micro-cooling, heating, and power (m-CHP) instructional module", Proquest,
26 words — < 1%